A

DISSERTATION REPORT

on

INVESTIGATION OF TOOL WEAR DURING FRICTION STIR WELDING OF METAL MATRIX COMPOSITES

Submitted in partial fulfillment of the requirements for the award of degree of

MASTER OF ENGINEERING

IN

CAD/CAM

Submitted by:

ASHISH BIST

ROLL NO: 801281006

Under the guidance of

Dr. O.P. Pandey	**Dr. J. S. Saini**	**Mr. Bikramjit Sharma**
Professor	**Asstt. Professor**	**Asstt. Professor**
School of Physics & Material Science	**MED**	**MED**

MECHANICAL ENGINEERING DEPARTMENT

THAPAR UNIVERSITY,

PATIALA-147004, INDIA

JULY-2014

ACKNOWLEDGEMENT

Though only my name appears on the cover of this dissertation, a lot of people have contribute to its completion. I owe my gratitude to all those people who have made this dissertation possible and because of whom my post graduate experience has been one that I will cherish forever.

My foremost and profound gratitude goes to my supervisor Dr. O. P. Pandey, Dr. J. S. Saini and Mr. Bikramjit Sharma for their proficient, enthusiastic guidance and encouragement. The suggestions have given by them undoubtedly helped in supplementing my thoughts in the right direction for attaining the desired objectives.

My heartfelt gratitude goes to Dr. Ajay Batish, Professor and Head, MED, for providing all the facilities required for the completion of my work.

I am also thankful to all the teaching and non-teaching staff members of mechanical engineering department who have contributed directly or indirectly towards the successful completion of my thesis.

My friends have helped me stay sane through these years. Their support and care helped me a lot. I would like to thank Mr. Ankit Thakur who helped me during my experimental work.

Most significantly, none of this would have been possible without the love and patience of my family. My parents to whom this dissertation is dedicated to, has been a relentless supply of love, concern, support and strength for these years.

All above, I express my indebtedness to thee “ALMIGHTY GOD” for all His blessings and kindness.

ASHISH BIST

Reg. No: 801281006

CERTIFICATE

I hereby declare that the dissertation entitled **"INVESTIGATION OF TOOL WEAR DURING FRICTION STIR WELDING OF METAL MATRIX COMPOSITE"** is an authentic record of my own work carried out in partial fulfillment of the requirement for the award of the degree of **Master of Engineering in CAD/CAM** under the guidance of Dr. O. P. Pandey. Professor, School of Physics and Materials Science, Dr. Jaswinder Singh Saini, Assistant Professor, Mechanical Engineering Department, Mr. Bikramjit Sharma, Assistant Professor, Mechanical Engineering Department, Thapar University, Patiala. The matter embodied in this report has not been submitted in partial or full to any other university or institute for the award of any degree.

Dated: 17.07.2014

(Ashish Bist)

(801281006)

It is certified that the above statement made by the student is correct to the best of my knowledge and belief.

Dr. O. P. Pandey
Professor
SPMS, Thapar University,

Dr. J. S. Saini
Assistant Professor
MED, Thapar University,

Mr. Bikramjit Sharma
Assistant Professor
MED, Thapar University,

(Countersigned by)

Dr. Ajay Batish
Professor and Head
MED, Thapar University,
Patiala (Punjab)-147004

Dr. S. K. Mohapatra
Dean of Academic Affairs
MED, Thapar University,
Patiala (Punjab)-147004

ABSTRACT

The metal matrix composites (MMCs) have received considerable attention in the world due to their excellent mechanical properties like higher strength, higher hardness, higher wear resistance etc. and because of these attractive properties, MMCs have been used in several applications like aerospace, marine, automotive etc. Friction stir welding (FSW) is preferred over conventional welding methods to achieve defect free welds for joining parts made of MMCs.

Wear of the welding pin tool, a consequence of prolonged contact between the tool and the harder reinforcements is the key issue for the FSW. The present work, wear in stir welding tool is studied by varying the process parameters (rotational speed, traverse speed and length of weld) while welding aluminum alloy, aluminum matrix composites.

TABLE OF CONTENTS

LIST OF TABLES

LIST OF FIGURES

ACRONYMS

Sr. No.	Abbreviations	Description
1.	FSW	Friction stir welding
2.	MMC	Metal matrix composite
3.	TWI	The welding institute
4.	HAZ	Heat affected zone
5.	TMAZ	Thermo-mechanically affected zone
6.	Al 359	Aluminum 359 alloy
7.	WC-Co	Tungsten-cobalt

CHAPTER 1 INTRODUCTION

1.1 COMPOSITE MATERIALS

Composite materials are engineered materials which exhibit improved and distinct properties in comparison to their constituents. One of the constituent is called matrix and the other one is called the reinforcing phase which is embedded into it. The reinforcing material may be in the form of fibers, particles or flakes. The matrix phase materials are continuous. It is possible to design a composite of desired mechanical properties and functional characteristics by combining these two materials in the right way. Metals and their alloys can't always meet the demands of today's advanced technologies. Only by combining several materials as in a composite one can meet the performance requirements.

1.1.1 CLASSIFICATION OF COMPOSITE MATERIALS

Composite materials are commonly classified into following two categories:

- Based on matrix constituent
- Based on reinforcement form

- **Classification based on matrix constituent**

(i) Metal Matrix Composites (MMCs)

MMCs are composed of a metallic matrix (aluminum, magnesium etc.) and a dispersed ceramics (oxides, carbides etc.) or metallic (lead, tungsten etc.) phase.

(ii) Ceramic Matrix Composites (CMCs)

CMCs are composed of a ceramic matrix and embedded fibers of other ceramic material (dispersed phase).

(iii) Polymer Matrix Composites (PMCs)

PMCs are composed of a matrix from thermoset (unsaturated polyester, epoxy) or thermoplastic (PVC, nylon, polystyrene) and embedded glass, carbon, steel or Kevlar fibers (dispersed phase).

- **Classification based on reinforcement form**

(i) Particulate Composite

Particulate composites consist of a matrix reinforced by a dispersed phase in the form of particles.

(ii) Fibrous composite

Fibrous reinforced composites consist of a matrix reinforced by a dispersed phase in the form of continuous or discontinuous fibers.

1.2 FRICTION STIR WELDING PROCESS

In late 1991 a very new and potentially good welding method was thought at TWI (The Welding Institute). The process was duly called Friction Stir Welding (FSW), and TWI registered for world-wide patent protection in December of that year. TWI which specializes in materials joining technology is a world famous institute in the UK. Consistent with the more conventional methods of friction welding, which had been practiced since the early 1950s, the weld was made in the solid phase, that is, no melting was involved. FSW used a rotating tool to generate the necessary heat for the process compared to conventional friction welding. Since its innovation, the process has received world-wide aid. It is also a cleaner and more effective process compared to conventional techniques.

1.2.1 Working principle

In FSW a cylindrical, shouldered tool with a profiled probe is rotated and slowly plunged into the joint line between two work pieces which are butted together. The parts have to be clamped onto a backing bar in a manner that prevents the abutting joint faces from being forced apart. This causes the generation of frictional heat between the wear resistant welding tool and the material of the work pieces. This heat causes the latter material to soften without reaching its melting point and allows traversing of the tool along the weld line. The maximum temperature achieved is of the order of 0.8% of the melting temperature of the material. The plasticized material is transmitted from the leading edge of the tool to the trailing edge of the tool probe and is forged by the intimate contact of the tool shoulder and the work piece. It create a solid phase bond between the two pieces. The schematic drawing of the Friction Stir Welding is shown in figure 1.1.

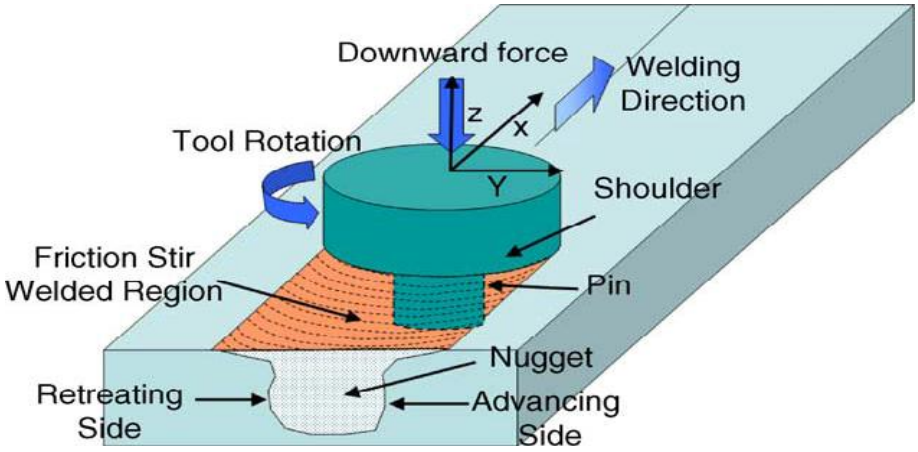

Figure 1.1 Schematic drawing of friction stir welding (Mishra and Ma, 2005)

1.2.2 Description of the rotating tool pin

The non-consumable tool has a circular section except at the end where there is a different profile probe (threaded or more complicated flute etc.) as shown in figure 1.2. The area between the cylindrical portion and the probe is known as the shoulder. The probe penetrates the work piece whereas the shoulder rubs with the top surface. The tool has an end tap of 5 to 6 mm diameter and a height of 5 to 6 mm (may vary with the metal thickness). The tool is set in a positive angle of some degree in the direction of welding. The design of the pin and shoulder of tool plays a major role in the material movement during the process and also effects the weld quality.

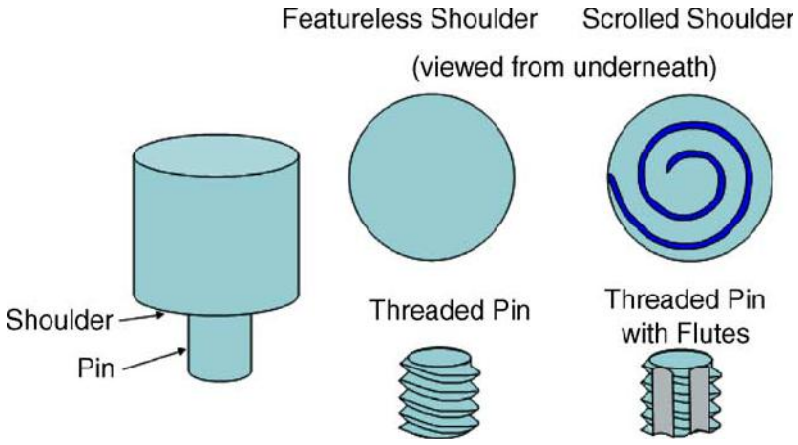

Figure 1.2 Schematic drawing of the FSW tool (Mishra and Ma, 2005)

1.2.3 Microstructure Classification

Threadgill (Threadgill, 2007) made the first attempt at classifying microstructures. The work was based purely on information available from aluminum alloys. However, it had become apparent from work on other materials that the behavior of aluminum alloys is not typical of most metallic materials, and therefore the scheme cannot be extended to cover all materials. It is therefore suggested that the following revised scheme is used. This has been originated at TWI, but has been accepted by the Friction Stir Welding Licensees Association. The system divides the weld zone into following four distinct regions as shown in figure 1.3:

(i) Unaffected material

(ii) Heat affected zone (HAZ)

(iii) Thermo-mechanically affected zone (TMAZ)

(iv) Weld nugget (Part of thermo-mechanically affected zone)

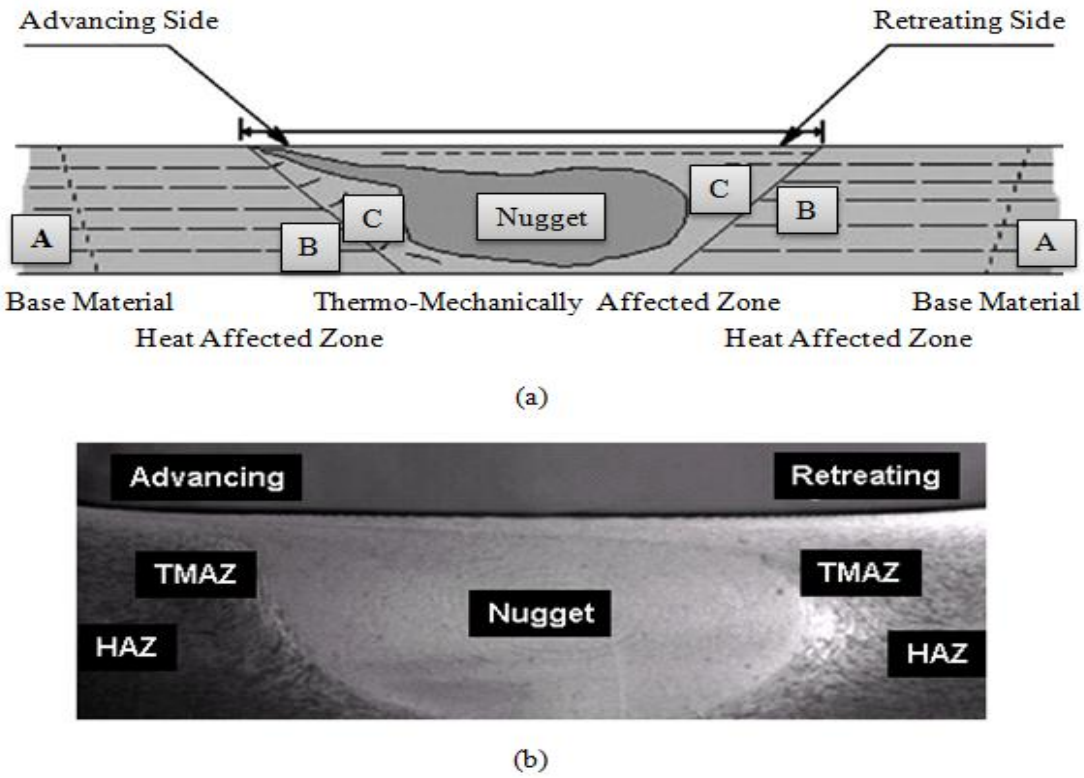

Figure 1.3 (a) Schematic diagram of micro structural zones in friction stir welds in Al (b) Micrograph showing various micro-structural zones (Threadgill, 2007)

(i) **Unaffected material or parent metal:** This is material far away from the weld, which has not been deformed, although it may have experienced a thermal cycle during welding. Also, weld is not affected by the heat in terms of microstructure or mechanical properties.

(ii) **Heat affected zone (HAZ):** In this region, which lies closer to the weld center, the material experience a thermal cycle, which modified the microstructure and/or the mechanical properties during the process. However, there is no plastic deformation occurring in this area. In the previous regions, this was referred to as the "thermally affected zone". The word ‘Heat Affected Zone’ is now preferred, as this is a direct parallel with the heat.

(iii) **Thermo-mechanically affected zone (TMAZ):** In this region, the material has been plastically deformed by the FSW tool, and the heat from the process will also have effect on the material. In the case of aluminum, it is possible to get substantial plastic strain without recrystallisation in this area, and there is generally a different boundary between the recrystallized zone and the deformed zones of the TMAZ. In the earlier classification, these two sub-zones were treated as different micro structural regions. However, subsequent work on other materials has shown that aluminum behaves in a different manner in comparison to most other materials, in that it can be extensively deformed at high temperature without recrystallisation. In other materials, the distinct recrystallized region (the nugget) is absent, and the whole of the TMAZ appears to be recrystallized.

(iv) **Weld Nugget:** Traditionally, the recrystallized area in the TMAZ in aluminum alloys has been called the nugget. Although this term is descriptive, it is not very scientific. However, its role has become widespread, and as there is no word which is equally simple with greater scientific merit, this term has been followed. A schematic diagram is shown in the above Figure 1.3 which clearly identifies the various regions. It has been suggested that the area immediately below the tool shoulder (which is clearly part of the TMAZ) should be given a distinguish category, as the grain structure is often dissimilar here. The microstructure here is decided by rubbing by the rear face of the shoulder, and the material may have cooled below its maximum. It is advised that this area is treated as a separate sub-zone of the TMAZ.

1.2.4 Factors affecting weld quality

The following are the different factors that affect the weld quality as shown in figure 1.4.

(i) Type of metal

(ii) Angle of tool

(iii) Traversing speed of the tool

(iv) Rotation speed of tool

(v) Pressure applied by the pin tool

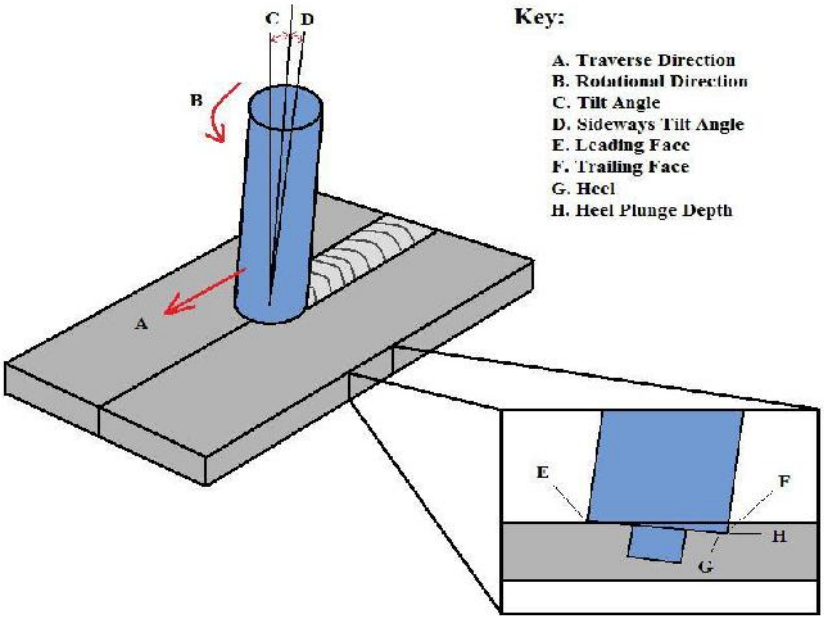

Figure 1.4 Diagram of FSW Tool Terms (Threadgill, 2007)

1.2.5 Joint geometries

The process has been used for the manufacture of weld joints like butt welds, overlap welds, T-sections, fillet, and corner welds as shown in figure 1.5. For each of these joint geometries particular tool designs are required which are being further developed and optimized. Fuel tanks for space flights with longitudinal butt welds and circumferential lap welds of Al alloy have been friction stir welded and successfully tested. The FSW process can also deal with circumferential, annular, non-linear, and three dimensional welds. Since gravity has no effect on the solid-phase welding process, it can be used in all positions like horizontal, vertical, overhead etc.

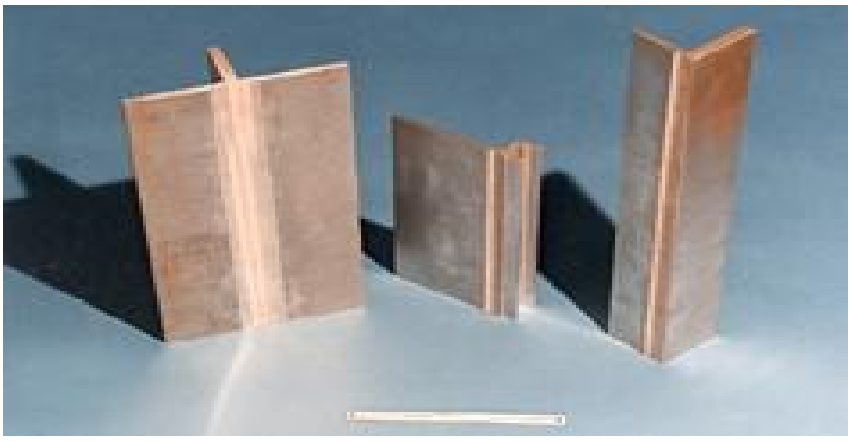

Figure 1.5 Different joint geometries (http://www.joining materials.html)

1.2.6 Friction Stir Welding - Advantages

The following are the main advantages of FSW:

(i) Since no fumes or spatter is generated and no shielding gas is required, so the process is environment friendly.

(ii) A non-consumable tool is used for the welding.

(iii) The process can be done in all positions like vertical, horizontal, or overhead, since the weld is obtained in solid phase, gravity does not play any part.

(iv) Since the temperature involved in the process is quite low, shrinkage of material during solidification is less.

(v) One tool can be used for up to 1000 meters of weld length (6000 series aluminum alloy).

(vi) No fusion or filler materials are required.

(vii) No oxide removal necessary as in fusion welding.

(viii) The weld obtained is of excellent mechanical properties with superior quality and fine micro structure.

(ix) Since mechanical forming after welding can be avoided, so the process is cost effective.

(x) Dissimilar metals can be welded.

(xi) Automation is possible.

1.2.7 Friction Stir Welding – Applications

FSW can be applied in nearly all the industries like shipbuilding, aerospace, railway etc.

(i) Shipbuilding and marine industries: The shipbuilding and marine industries are two of the first industry areas which have adopted the FSW process for commercial applications. The following figure 1.6 shows the aluminum ship constructed using FSW in Japan. The process is suitable for the following applications:

- Aluminum extrusions.
- Panels for decks, sides, bulkheads and floors.
- Marine and transport structures.
- Masts and booms, e.g. for sailing boats.
- Helicopter landing platforms.
- Offshore accommodation.

Figure 1.6 Aluminum ships constructed in Japan using FSW (Rowe and Thomas, 2006)

(ii) Aerospace industry: At present the aerospace industry is using friction stir welding for welding of prototype parts. Also, Opportunities exist to weld skins to spars, ribs, and stringers for use in military and civilian aircraft. This offers significant benefits compared to riveting and machining from solid, such as reduced manufacturing costs and weight savings. Longitudinal butt welds and circumferential lap welds of aluminum alloy fuel tanks for space vehicles have been welded by FSW and successfully tested. The process

could also be used to increase the size of commercially sheets available by welding them before forming. The FSW process can therefore be considered for:

- Aviation fuel tanks.
- Cryogenic fuel tanks for space vehicles as shown in figure 1.7.
- Repair of faulty MIG welds.
- Wings, fuselages.
- External throw away tanks for military aircraft.
- Military and scientific rockets.

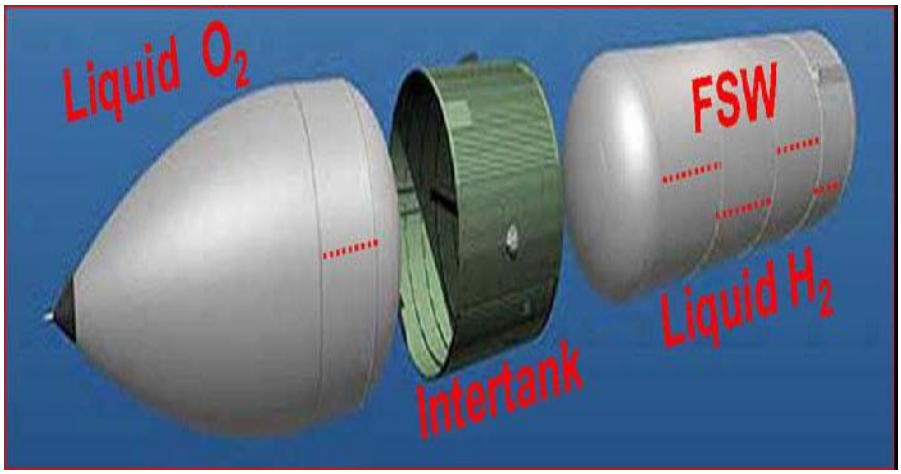

Figure 1.7 Rocket fuel tanks fabricated by FSW (Rowe and Thomas, 2006)

(iii) Railway industry: FSW joined the commercial produced high speed trains made from aluminum extrusions has been published. Figure 1.8 shows the Japanese railway rolling stock which used the FSW process. Applications include:

- Railway tankers and goods wagons.
- Rolling stock of railways, underground carriages, trams.
- High speed trains.
- Container bodies.

Figure 1.8 Japanese railway rolling stock fabricated from aluminum by FSW (Rowe and Thomas, 2006)

(iv) Land transportation: The FSW process is currently being experimentally assessed by many automotive companies and suppliers to this industrial sector for its commercial application. A joint EWI/TWI Group Sponsored Project is investigating representative joint designs for automotive lightweight structures. Potential applications are:

- Fuel tankers.
- Engine and chassis cradles.
- Wheel rims.
- Space frames, e.g. welding extruded tubes to cast nodes.
- Truck bodies.
- Motorcycle and bicycle frames.
- Mobile cranes.
- Buses and airfield transportation vehicles.
- Tail lifts for lorries.
- Articulated lifts and personnel bridges.

(v) Construction industry: The use of portable FSW equipment is possible for:

- Window frames.
- Aluminum bridges.
- Aluminum pipelines.

- Aluminum reactors for power plants and the chemical industry.
- Heat exchangers and air conditioners.
- Pipe fabrication.

(vi) Electrical industry: The electrical industry shows increasing interest in the application of FSW for:

- Electrical connectors.
- Electric motor housings.
- Encapsulation of electronics.

(vii) Other industry sectors: Friction stir welding can also be regarded for:

- Gas tanks and gas cylinders.
- White goods.
- Refrigeration panels.
- Cooking equipment and kitchens.
- Connecting of aluminum or copper coils in rolling mills.
- Furniture.

1.2.8 Friction Stir Welding – Limitations

The FSW has following limitations:

(i) Keyhole at the end of each weld due to pin of tool.
(ii) Welding speeds are moderately slower.
(iii) Work pieces must be rigidly clamped for defect free weld.
(iv) Backing bar required.
(v) Requirement of different length pin tools when welding materials of varying thickness.

CHAPTER 2 LITERATURE REVIEW

The significant effort has been done in transferring the technological benefits of FSW from aluminum to other materials. Attempts are on to make the process more flexible. In the new millennium there is no doubt that the automotive sector, aerospace industry, marine industry etc. will find an increasing use of this process because of its lower cost and ability to weld dissimilar material combinations with minimal distortion. The process has been an excellent substitute for composites that have joining problem arising from fusion welding.

2.1 Friction Stir Welding (FSW) Process

Thomas *et al*. (1991) documented that FSW was a joining technique developed by The Welding Institute (TWI) of Cambridge, England in 1991. **Friction Stir Welding, Space Shuttle Technology Summary (2001), NASA** published that a significant benefit of FSW was that it had significantly fewer process elements to control. In a Fusion weld, there were many process factors that must be controlled–such as purge gas, voltage, wire feed, travel speed, shield gas, arc gap. However, in Friction Stir Weld there were only four process variables to control: rotation speed, travel speed, tilting angle and downward pressure. The increase in joint strength combined with the reduction in process variability provides for an increased safety margin and high degree of reliability for the External Tank. **Sidhu and Chatha (2012)** investigated the main process parameters and there effects in friction stir welding. The rotational speed helped in stirring, mixing of material and generating the frictional heat, welding speed controls the heat as well as reason of appearance of weld generated, downward force helps in maintaining contact conditions and generates the frictional heat and the tilting angle helps in thinning and appearance of the weld. **Palanivel *et al.* (2012)** studied that the welding speed prompted the translation of tool which in turn pushes the stirred material which arises due to the tool rotation from front to the back of the tool pin and completes the welding. The rubbing of tool shoulder and pin with the work piece generated the frictional heat. A fully coupled thermo-mechanical model is adopted to study the effect of shoulder size on the temperature distributions and the material deformations in FSW. Numerical results indicate that the maximum temperature can be increased with the increase of the shoulder diameter. The stirring zone can be enlarged by the increase of the shoulder size **(Zhang *et al.*, 2009).** It is observed that increasing rotational/traverse speed (ω/v)

ratio increases the weld nugget size and decreases the incomplete root penetration. By increasing ω/v, a slight decrease in the effective tensile properties calculated from shear punch test (SPT) of different zones is observed. That is due to increased heat input and softening of the material in these regions. Furthermore, increasing ω/v ratio results in the formation of a larger weld nugget because of an increase in heat input and an easier material flow. Therefore, the probability of formation of ‘‘incomplete root penetration’’ defect is reduced when ω/v ratio increases **(Gharacheh *et al.*, 2006)**.

2.2 Comparison of FSW Process with other welding processes

FSW is very much preferred for joining unweldable aluminum alloys such as the 2xxx and 7xxx series used in aircraft structures. The strength of the weld is 30%-50% higher than with arc welding. The fatigue life is comparable to that of riveted panels. Boeing made a $15 million investment in the use of FSW to weld the booster core tanks for the Delta range of space launch vehicles, which is the first production FSW in the USA. The first launch of a FSW tank in Delta II rocket happens in August 1999. This process is also considered for the joining of aluminum–beryllium alloys such as 2195 for the central tank of the Space shuttle and also titanium alloys for other aeronautical uses. As FSW becomes better establish, it can replace Plasma Arc Welding (PAW) and Electron Beam Welding (EBW) in some specific applications in aluminum and titanium respectively **(Patricio *et al.* 2000)**. The comparison of the FSW process with other processes like Gas Tungsten Arc Welding (GTAW), Gas Metal Arc Welding (GMAW) and Laser Beam Welding (LBW) is done. FSW is used to weld different materials such as wrought aluminum alloy, magnesium alloy, IF steel, mild steel and stainless steel. The wrought aluminum alloy joints fabricate by FSW exhibits higher strength values which are approximately 34% higher compared to the GMAW joints and 28% higher compared to the GTAW joints. The magnesium alloy joints fabricated by LBW exhibits higher strength values which are 14% compared to GTAW joints and 2% compared to FSW joints, but LBW process is costly as compared to FSW. The IF steel joints fabricated by FSW process exhibited higher strength values and the enhancement in strength was approximately 24 % compared to joint fabricated by GTAW process **(Balasubramanian 2010)**. FSW can potentially replace the riveting and resistance spot welding of aluminum and steel sheets in the aircraft and automotive industries, respectively **(Biswas *et al.* 2009).**

2.3 Metal matrix composite produced by Stir Casting Method

Kunze and Bampton (2001) reported that Metal-Matrix Composites (MMCs) had received considerable attention over the past 30 years due to their attractive strength, stiffness, fatigue, and thermal properties. Aerospace industry goals had called for reduced weight in both space-propulsion systems and space structures. MMCs offered several potential benefits to help the industry meet this goal. These benefits included high specific strength and stiffness, low Coefficient of Thermal Expansion (CTE), often coupled with good thermal conductivity and low density and the potential to tailor properties for a specific application. As a result of these attractive properties, MMCs had been used in several important space-based applications, including structural tubes for the Space Shuttle Orbiter, the antenna waveguide mast for the Hubble Space Telescope, and for thermal management in satellite communication devices. Metal Matrix Composite (MMC) is engineered combination of metal (Matrix) and hard particles (Reinforcement) to tailored properties. **Hashim *et al.* (1999)** documented that the addition of high strength, high modulus refractory reinforcement particles to a ductile metal matrix produces a material whose mechanical properties are intermediate between the matrix alloy and the reinforcement. Aluminum and silicon carbide, for example, have very different mechanical properties: Young's moduli of 70 and 400 GPa, coefficients of thermal expansion of 24 x 10^{-6} and 4 x $10^{-6}/^{o}$C, and yield strengths of 35 and 600 MPa, respectively. By combining these materials, e.g. A6061/SiC/17p (T6 condition), an MMC with a Young's modulus of 96.6 GPa and a yield strength of 510 MPa can be produced. **Prabu *et al.* (2006)** reported that in recent years many processing techniques have been developed to process particulate reinforced metal matrix composites. According to the type of reinforcement, the fabrication techniques can vary considerably. These techniques are stir casting, liquid metal infiltration, squeeze casting, spray decomposition and powder metallurgy. Among the variety of processing techniques available for particulate or discontinuous reinforced metal matrix composites, stir casting is one of the methods for the production of large quantity commercially practised. It is attractive because of flexibility, simplicity and most economical for large sized components to be fabricated. **Singla *et al.* (2009)** documented that the cost of preparing composites material using a casting method is about one-third to half that of competitive methods available, and for high volume production, it is projected that the cost will fall to one-tenth. **Sharma *et al.*** studied that in a stir casting process, the reinforcing phases (usually in powder form) are distributed into molten Aluminum by

mechanical stirring. Stir casting is suitable for manufacturing composites with up to 30% volume fractions. The distribution of the particles in the molten matrix depends on the geometry of the mechanical stirrer, stirring parameters, placement of the mechanical stirrer in the melt, melting temperature, and the characteristics of the particles added.

2.4 Metal matrix composite joints produced using FSW

Weld ability of these composites are significantly reduced due to the addition of ceramic reinforcements. It is hard to achieve defect-free MMC welds. The drawbacks associate with the fusion welding include: (a) the incomplete mixing of the parent and filler materials, (b) the presence of porosity as large as 100 μm in the fusion zone, (c) the excess eutectic formation and (d) the formation of undesirable deleterious phases such as Al_4C_3 **(Storjohann *et al.*, 2005)**. It is generally known that the fusion-welding processes often leads to the deterioration of these metal-matrix composites. In the case of Al_2O_3 reinforced composites, the Al_2O_3 decomposes to aluminum and gas on contact with liquid aluminum **(Ellis *et al.*, 1994).** Similarly, in the case of SiC-reinforced composites, the SiC reacts with molten aluminum to form Al_4C_3 carbide **(Iseki *et al.*, 1984).** The literature shows that the tendency toward the formation of Al $_4C_3$ can be reduced in certain arc welding conditions **(Ellis *et al.*, 1994).** During laser welding, it is very difficult to avoid these decompositions. However, **Dahotre *et al.* (1991)** showed that decreasing the specific energy during laser melting could reduce the formation of Al_4C_3. These defects can be reduced or eliminated through careful control of the heat input which a solid-state joining process such as FSW was a more viable alternative **(Storjohann *et al.*, 2005)**.

2.5 Wear of FSW tools in the joining of MMCs

Prater *et al.* (2008) documented that tool wear in FSW was an undesirable feature because erosion of the probe features and/or probe length inhibited the flow of material (particularly in the vertical direction), which in turn increased the likelihood of defect formation. For instance, a reduction in the length of the probe as a consequence of wear often created a lack of consolidated material (void) at the base of the joint known as the root flaw defect. **Prater (2011)** concluded that while FSW tools made from conventional materials had a nearly infinite life when used to join Aluminum alloys, they exhibited wear in the welding of harder materials such as metal composites and steel**. Prater *et al.* (2013)** reported that the challenge in the welding of MMCs using FSW was thus to maintain wear below an experimentally determined threshold where the

probability of defect formation became unacceptable and, in instances where deterioration couldn't be confined to the low-wear regime over the course of the weld, and to replace the tool before it attained this critical value of wear. The amount of wear a particular tool would experience during an MMC weld was hypothesized to vary inversely with the hardness ratio H, a dimensionless metric defined as the hardness of the tool (H_t) material to that of the reinforcement (H_r). When H was less than 1, the hardness of the reinforcement exceeded the hardness of the tool ($H_r > H_t$). For these cases, an increase in the hardness ratio (accomplished by decreasing the hardness of the reinforcement or increasing the hardness of the tool) should correspond to a proportional decrease in the amount of wear the tool experiences. Tool wear couldn't occur when the hardness ratio was greater than 1, as the hardness of the tool was greater than that of the reinforcing material ($H_t > H_r$).

2.6 Quantifying wear of tool

The tool material eroded as a result of contact with hard reinforcing particles is deposited along the joint line. This abraded material can be detected and quantified. **Prater, 2011**; **Fernandez and Murr, 2004** measured wear by capturing close-up photos of the tool probe, cutting out the probe in these images, and comparing the weights of the cutouts. The assumption that the weight of the two-dimensional image cutout is indicative of the tool's material loss is substantiated by a series of parallel experiments which calculate percent wear by comparing masses of the etched tool after each weld. In order to quantitatively assess the tool wear, **Liu *et al.* (2005)** use the percent variation in tool size as evaluation index (equation (1)).

$$Variation = \frac{(original\ size - measured\ size)}{original\ size} \times 100\ \% \qquad (1)$$

At the completion of each weld **Prater *et al.* (2010)** mount the tool in an optics bench and close-up images of the probe are taken using a Canon A620 Power shot camera. These images are imported into the imaging software, where the wear of the probe is quantified by comparing pre-weld images of the probe with those taken after a given weld traverse distance. The percent tool loss is calculated using equation (2).

$$Percent\ tool\ loss = \frac{(P - P_I)}{P} \times 100\ \% \qquad (2)$$

where, P represents the original pixel count of the probe,

P' represents the probe's pixel count after some weld distance.

A 1 cm square grid fixed behind the tool is used to convert measurements from pixels to square centimeters. **Hassan *et al.* (2012)** use an electronic digital balance with 0.1 mg accuracy to measure the initial and final mass of the specimen. The masses of all specimens are measured before and after running. The test is carried out for three hours; then the specimens are removed from the wear testing machine and cleaned with alcohol, in order to remove all the attached worn particles, and then the mass of the specimen is measured to determine the mass loss. The wear rates are determined using the volume loss method, as indicated by the following equation (3).

$$W = \frac{M}{\rho \times s} \quad (3)$$

where W = volume loss during test period (cm^3/m),

M = mass loss during wear test (g),

s = sliding distance (m),

ρ = density of the composite as computed from the rule of mixture = 2.7 g/ cm^3.

Prater *et al.* (2013) quantify the wear by measuring changes in the weight of the probe inserts as a result of wear (inserts are removed after each weld, analyzed, and re-inserted prior to the next experiment in the series because aluminum accumulates on the probe surface during welding, inserts must be etched prior to analysis. The insert is immersed in a solution of NaOH and water until all the aluminum is eroded from the surface.). Percent wear is calculated from equation (4).

$$Percent\ wear = \frac{mi - \Delta m}{mi} \times 100\,\% \quad (4)$$

where mi denoted the initial mass of the probe,

Δm was the change in mass of the probe insert.

Prater *et al.* (2013) use Nunes's rotating plug model to develop a model of tool wear in FSW of MMCs. The rotating plug model for wear in FSW of MMCs yields an expression (equation (5)).

$$Percentage\ wear = \frac{5D\Delta C_{max}P\omega l}{24Rv}\% \quad (5)$$

where D is mean diameter of abrasive particles of MMC reinforced,

ΔC_{max} is maximum cutting arc,

P is volume of abrasive particles of MMC reinforced,

ω is rotational rate,

l is distance welded,

R is probe radius of tool,

v is traverse speed

which can be used to estimate the percent wear incurred by the FSW probe in joining an MMC.

2.7 Relationship between wear and process parameter

Prado *et al.* (2001) investigated the tool wear behavior in FSW of Al_2O_3p/6061Al composite. For O1 tool-steel threaded pin, heat-treated to an Rc hardness of 62, at a tool rotation rate of 500-2000 rpm and a traverse speed of 60 mm/min, while no apparent tool wear was noted for FSW of 6061Al, severe tool wear occurred for FSW of Al_2O_3p /6061Al composite. The wear rate of the tool increased linearly with increasing linear welding distance. The largest wear rate was observed at a tool rotation rate of 1000 rpm. This means that the wear rate of tool did not increase when the tool rotation rate was increased above 1000 rpm. A possible reason for this is the improvement of flow properties of the composite at high tool rotation rate due to increased thermal input. An investigation published by **Prado *et al.* (2003)** provides a preliminary assessment of the wear of cylindrical threaded tools in the butt welding of Al 6061/ Al_2O_3p/20p. **Prado *et al.* (2003)** observed that tool wear and the rate of wear for hardened, steel, right-hand screws rotating at 1000 rpm in the friction-stir welding of Al 6061+20 vol.%Al_2O_3 particles were observed to decrease for increasing weld or traverse speeds. An optimized tool shape emerged, when sufficiently long traverse distances were reached, tool wear became small or negligible. This shape was slightly different at 6 and 9 mm/s traverse speeds but in each case a self-optimized tool shape emerged. This self-optimizing wear phenomena and tool shape result by counter motions of solid-state flow regimes which depend upon both actual traverse speed and tool rotation speed. Although sound, porosity-free welds were obtained with both the unworn, threaded pin tool and the worn, unthreaded pin tool, microstructures vary and the worn pin tool produced a narrower heat affected zone with less drop in hardness than the threaded pin tool. Data reported in an analogous study by **Fernandez and Murr (2003)**, which considers butt welds of Al 359/SiC/20p, supported a similar conclusion. Wear in this process could be controlled to a limited extent through careful selection of process parameters. The relationship between wear and process parameters in FSW of MMCs had been studied extensively by **Prado *et al.* (2003) and Prater *et al.* (2010)**, respectively. **Prater (2013)** concluded that the amount of volumetric wear experienced by a tool in FSW of MMCs was directly proportional to rotation rate and distance welded but inversely proportional to traverse speed. The parameters which minimize wear (low rotation rates coupled with high traverse speeds) were not necessarily the

same parameters capable of producing welds with mechanical properties deemed acceptable for a specific application. Even at parameters in the low-wear regime, the cumulative wear of the tool over long distances would eventually necessitate its replacement. Thus, mitigation of wear through process parameters might only be feasible over shorter weld distances in noncritical applications. **Prater (2011)** studied that once a robust method of wear measurement had been established; the variation of wear with process parameters can be investigated. The wear experiments detailed in references related the volumetric wear of the probe to the process parameters rotation speed (ω), travel speed (ν) and distance welded (l).Though the studies utilized different metal composite materials and tool geometries, there were some trends that seemed to hold in general for FSW of MMCs. An obvious direct proportionality between wear and linear weld distance was reported in all studies. In particular, **Liu *et al.* (2005)** noted the dramatic reduction in the diameter of the probe with increasing weld length. An appreciable tool wear was observed in the FSW of AC4AC30 vol% SiCp AMC although the threaded tool was made of WC–Co hard alloy was used at the tool rotation rates of 1500-2000 rpm and the traverse speeds of 25-150 mm/min. The shoulder size and pin length were changed slightly and the radial wear of the pin was most severe for the whole tool. The radial wear of the pin was very different at different locations of the pin, and the maximum wear was finally produced at a location of about one-third pin length from the pin root. The welding speed had a decisive effect on radial wear rate of the pin. The lower the welding speed, the higher the wear rate and the maximum wear rate was produced in the initial welding. For example, after an initial welding was performed at a welding speed of 25 mm/min, the pin diameter decreased at most by 11%. After the seventh welding was performed, 27% of the pin diameter at the maximum-wear location disappeared. In addition, **Prado *et al.* (2003) and Shindo *et al.* (2002)** found that the tool wearing in the FSW process of Al_2O_3p/6061Al and SiCp/359Al composites produced a self-optimized shape which resulted in excellent welds and no additional tool wear when that was achieved. This provided a new idea for the geometry design of the welding tool. **Shindo *et al.* (2002)** proposed that the FSW of Al359+20% SiC MMC using threaded steel pin tools for welding produces a self-optimized shape with no threads which continued to produce excellent, homogeneous welds, but without additional tool wear or shape change at fixed welding speeds above 6 mm/s. This self-optimized shape was slightly different at 6 mm/s and 9 mm/s. Extrapolations of linear wear rate data indicated zero wear rate above about 11 mm/s weld speed.

To isolate the effect of rotation speed on wear, **Fernandez and Murr (2004)** performed welds at a fixed traverse rate while varying the spindle speed from 500 rpm to 1000 rpm. The percent tool wear increased with increasing rotation speed. This trend is also observed by **Prado *et al.* (2001)** who found that wear increased with rotation speed up to 2000 rpm. To characterize the dependence of wear on traverse rate, **Fernandez and Murr (2004)** expanded their experimental matrix to include variations in traverse speeds. The wear curves for the seven combinations of traverse and rotation speeds considered were plotted. By comparing wear data for parameter sets with the same rotation speed but different traverse rates, it was apparent that wear decreases with increasing traverse speed. Though the inverse relationship between wear and traverse rate was nonintuitive, it provided experimental evidence that tool wear in the FSW process was a shear, rather than drag, phenomenon. **Prater *et al.* (2010)** used a Taguchi L27 orthogonal array for the characterization of Tool wear for various process parameters in the Friction Stir Welding of the Metal Matrix Composite Al 359/SiC/20p. The tool geometry selected for the experiment was the Trivex, an approximately triangular probe shape which arose from the CFD modeling work of TWI researchers **Shercliff and Colegrove (2006)**, who found that it was effective in reducing traversing forces by 18 to 25 percent and the axial force by as much as 12 percent. The surfaces of the probe were convex and the three vertices, when connected, form an equilateral triangle. Each vertex was located at the center of a circle which contained the other two vertices. The steel Trivex tools used in this study had a swept diameter of 0.25" and a probe length of 0.185"; the shoulder diameter was 0.75". Samples were welded at a 1^0 angle of tilt with a plunge depth of 0.009".Three factors (rotation speed, traverse rate, and length of weld) were correlated with a single outcome variable, percent tool wear. The multiple regression model ($W = 0.584 \times l - 1.038 \times \nu - 0.009 \times \omega - 6.028$ with an R^2 value of 0.81) indicated that wear was strongly dependent on process parameters. This relationship was of the form $W \propto \omega \times l/\nu$, where percent total tool wear (W) was inversely proportional to traverse rate (ν) (inches per minute) and directly proportional to rotation speed (ω) (rpm) and length of weld (l) (inches). **Sinclair *et al.* (2010)** investigated the effect of preheating on process forces of FSW. The weld samples were plates of A6061-T6 aluminum, nominally 0.250" thick, 3" wide, and 9" long. The FSW tool was made from H-13 tool steel heat treated to RC 48-50. It featured a 0.625" diameter shoulder and 0.250" side-length Trivex pin ground down to be 0.237" long. Based on previous work the tool was put on a 1^o tilt angle and 0.0074" plunge depth to achieve 80%

shoulder contact; all this geometry combined to give a joint ligament of just under 0.01". Overall the heating of the aluminum with an additional source beyond the FSW tool had definitely reduced the major process force associated with this new type of welding. With even small amounts of heating, the average axial force of welding AA6061 at some temperature dropped by a minimum of 21% for all welding traverse speeds. The maximum reduction seen was a great 43% reduction in force. The difficulties with higher strength material FSW had prompted a look into how to reduce the forces experienced by the tool. This goal had a number of sought-after benefits: reduced tool wear and clamping forces, allowing faster travel speeds, and even lower energy consumption. One way this was accomplished is with more advanced tool designs, such as the development of the Trivex pin by TWI. Thinking another way, by adding even slight preheating capabilities the travel speed or tool life of FSW could be significantly improved. If a tool was shown to have good wear characteristics under a certain load, the allowable travel speed could be easily doubled or almost tripled with additional energy input. The force-control welds supported this last point in the strongest possible way. **Hassan *et al.* (2012)** joined the aluminum matrix composites reinforced with both SiC and graphite particles using a FSW process. The wear characteristics of the welded joints were investigated at a rotational speed of 1,000 rpm and constant load of 50 N using a pin-on-disk wear testing apparatus. **Hassan *et al.* (2012)** focused on the influences of the FSW processing parameters like tool geometry, rotational speed, and welding speed on the wear characteristics of the produced welded joint of the considered hybrid aluminum matrix composite under dry sliding conditions. The experimental results indicated that the wear resistance of the joint increased at high welding speeds (>45 mm/min) and/or low value of rotational speeds. Different tool pin profiles (square, octagonal, and hexagonal) were developed to perform the welding process and the effects of the tool pin profile on the weldments were studied. It was found that joints welded with square pin profile had better wear resistance compared to the other pin profiles. **Palanivel *et al.* (2012)** considered the four FSW parameters for experiments *i.e.* tool pin profile, tool rotational speed, welding speed and axial force. Five different tools made of high carbon steel (HCHCr) of different tool profiles of straight, square, tapered square, straight hexagon, straight octagon and tapered octagon are used for FSW of dissimilar AA5083H111-AA6351 T6 aluminum alloy. Analysis of Variance (ANOVA) technique had been used to check the adequacy of the developed model. The experiment result showed that wear resistance increased as tool rotational speed increases and reaches to maximum

at 950 rpm. Further increase in tool rotational speed leads to decrease in wear resistance. Increase in frictional heat generation was observed with increase in tool rotational speed. Lower and higher heat input condition prevailed at lower (600 and 775 rpm) and higher (1125 and 1400 rpm) tool rotational speeds. Lower heat generation was also associated with lack of stirring and higher heat condition release excessive stirred materials. Micro level voids appeared at higher tool rotational speed which leads to poor wear resistance. Similarly, increase in welding speed gave rise to increase in wear resistance also and reached to maximum at 63 mm/min. Further increase in welding speed leads to decrease the wear resistance. The wear resistance increased as axial force increased and reached maximum at 1.25 tones. Further increase in axial force leads to decreased wear resistance. Low heat was generated at low axial force (1 and 1.25 tones) as well as caused improper consolidation of material and micro voids appeared lead to poor wear resistance. Higher heat was generated, plunge depth of the tool into the welded plate was higher and flash level which caused local thinning of welded plate leading to poor wear resistance increased at higher axial forces (1.75 and 2 tones). Tool pin profile played a crucial role in material flow during welding. The relationship between the static and dynamic volume of the tool pin decided the path for the flow of plasticized material from the leading edge to the trailing edge of the rotating tool. The square pin profile hexagon pin profile and octagon pin profile produced 63 pulses/sec, 95 pulses/sec, 126 pulses/sec respectively when the tool rotated at a speed of 950 rpm. There was negligible pulsating action in the case of octagonal and hexagonal pin profiled tool because it almost resembled a straight cylindrical pin profiled tool at this high rpm. The tapered pin profile tools were ineffective to produce pulsating stirring action. Hence the joints fabricated using straight pin profiles yielded highest wear resistance. The maximum achievable wear resistance had been taken from the apex of the response surface graph. By analyzing the response surfaces and contour plots the maximum achievable wear resistance value was found to be 244.693 m/mm^3. The corresponding FSW parameters that yielded this maximum value were tool pin profile of straight square tool, tool rotational speed of 950 rpm, welding speed of 63 mm/min and axial force of 1.5 tonne. **Prater *et al.* (2012)** developed a dimensionless parameter which could be used to estimate the amount of volumetric wear, a friction stir welding tool would experience in joining a metal matrix composite. Metal matrix composites were strong, lightweight materials consisting of a metal matrix (often an aluminum alloy) reinforced with ceramic particles or fibers. The study derived a dimensionless number based on three major

process variables in friction stir welding: rotation speed, traverse speed, and length of weld. This number was correlated with wear data collected from experiments in which a steel friction stir welding tool was used to join Al 359/SiC/20p. The use of the dimensionless number as a classifier for tool condition was also evaluated. **Prater *et al.* (2013)** evaluated the effectiveness of harder tool materials to combat wear in the FSW of MMCs. The tool materials considered were O1 steel, cemented carbide (WC-Co) of the micrograin and submicrograin varieties, and WC-Co coated with diamond for two MMCs i.e. Al 359 (T6 temper) with 20% SiC (by volume), and Al 359 containing 30% SiC. The challenges which accompany the application of harder tool materials and diamond coatings in FSW were also discussed. The study represented the first use of diamond-coated tools in FSW and the first comparative evaluation of tool materials for this application. The wear resistance of tools in FSW of MMCs was subjected to a law of diminishing returns. Increasing the hardness ratio from 0.31 (the value associated with O1 tool steel) to 0.77 (cemented WC-Co) produced a very substantial decrease in wear of the probe (somewhere in the 60-80% range, depending on reinforcement level). Increasing the hardness ratio beyond this (from 0.77 to 2.69) by applying a diamond coating produced a comparatively smaller proportional decrease in wear. An important finding of this study was that the relationship between wear and percentage reinforcement was not 1 to 1. To illustrate this point, close-up images of probe profiles prior to welding and after completing the series of Al MMC welds with either 20 or 30% reinforcement were compared in for the steel, WC/Co micrograin, WC/Co submicrograin, and diamond- coated inserts, respectively. The difference in wear with percentage reinforcement for WC/Co and the diamond-coated specimens was very subtle.

2.8 Conclusion from the literature review

Following are the points which can be concluded from the literature review:

- FSW occurs below the melting point of the workpiece, therefore reaction producing the theta phase doesn't occur. The absence of theta phase produces MMC joints that are stronger than their fusion welded counterparts.
- The stirring action of the FSW tool results in a redistribution of reinforcement particles, producing the "optimal microstructure," a characterization that reflects a refined grain structure exceeding that present in the parent material.

- FSW of MMCs is complicated by rapid and severe wear of the tool, a result of contact between the tool and the much harder reinforcement particles. The amount of wear incurred by the tool in FSW of MMCs is thought to dependent on several factors: the hardness of the tool relative to the reinforcement material in the composite, the composite's percent reinforcement, and the processing parameters. Most studies on wear have focused on the latter. In general, the total amount of material removed from the tool is in direct proportion to the rotations speed of the tool and the length of the joint but inversely proportional to traverse rate.
- Different methods have been developed for the quantification of tool material erosion which help in finding the relation between the wear and the process parameter.
- An understanding of the wear mechanism is essential for determining effective methods to combat wear. The development of wear-resistant tools is necessary to make solid-state joining of MMCs cost effective by eliminating the expenses associated with consumable tooling.

  The ultimate goal of present work is twofold: to produce repeatable, robust welds while simultaneously minimizing the frequency of tool replacement.

2.9 Gaps in the literature review

Some of the gaps in the literature review are given below:

- Less amount of work is reported on FSW of hybrid composites.
- Relation of wear with the parameters other than rotational speed, traverse speed and length of weld has not been addressed.
- Comparison of wear of FSW tool in case of alloy, composite and hybrid composite is still to be studied.

2.10 Problem formulation

Tool wear in FSW is an undesirable feature as it ultimately affect the weld formation during the process. Different methods have been applied for the quantification of tool wear. This wear is ultimately related to different process parameters of the process. So, the present work is to study the different process parameters on which the tool wear depends in FSW. The main objectives of proposed work are listed below:

(i) Preparation aluminum metal matrix composites containing different concentration of SiC and graphite for investigation.

(ii) Evaluation of metallurgical (SEM with EDS) and mechanical characteristics (Micro and Macro hardness) of produced MMCs (before friction stir welding).

(iii) Selection of appropriate test matrix of parameters for the experiment.

(iv) Joining MMCs using FSW using different combination of process parameters.

(v) Studying the effect of process parameters on tool wear.

(vi) Validation of Maximum temperature of welded portion and shoulder of tool.

(vii) Studying the effect of FSW parameters on micro hardness of welded plates.

CHAPTER 3 EXPERIMENTAL PROCEDURE

3.1 Preparation of Composite material

3.1.1 Materials

As a matrix material, Aluminum alloy was used. Aluminum alloy was selected because of its properties like high corrosion resistance, excellent machining properties, light weight and high ductility. Al 359 alloy is mostly used in aerospace industry. 20 kg of Al 359 has been purchased from Sohan Singh Moulding Industries, Yamuna Nagar. For the reinforced material SiC and graphite powder has been selected. SiC is hard material with high strength, high wear resistance, and low thermal expansion. Graphite powder is used as it improves the machinability and wear resistance of the considered composite. Graphite acts as a lubricating agent also. Both SiC and Graphite powder are purchased from Shanker & Co., New Delhi.

To determine actual composition of Aluminum 359 alloy, scanning electron microscopy was done in SAI lab, Thapar University, Patiala (figure 3.1). The machine and its results are shown in figure 3.1 and 3.2.

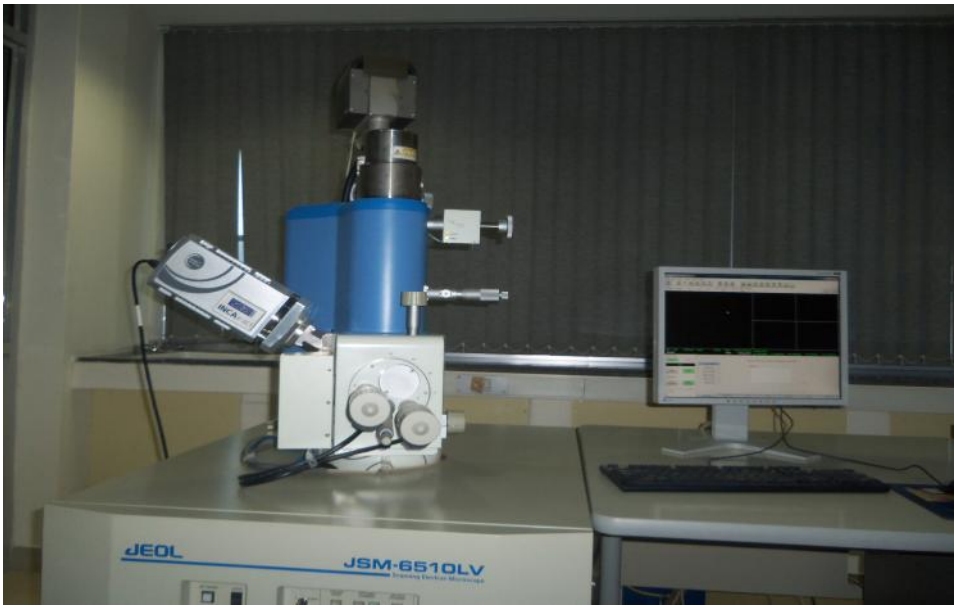

Figure 3.1: Scanning Electron Microscope (SEM) machine

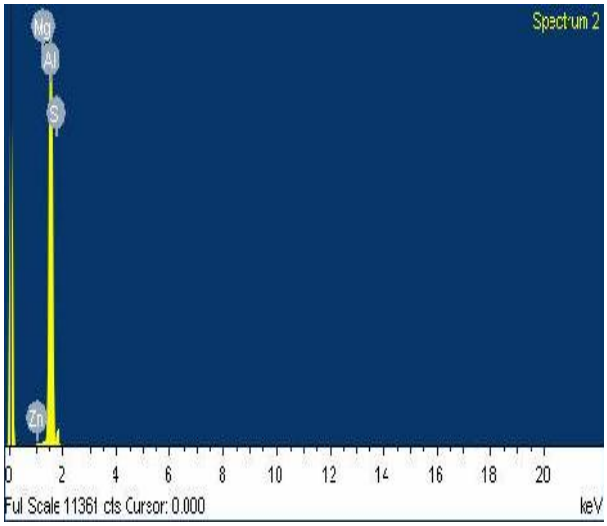

Element	Weight%
Al K	86.97
Si K	10.22
Fe K	1.39
Mn K	0.47
Zn K	0.38
Cu K	0.30
Ti K	0.17
Mg K	0.11
Totals	100.00

Figure 3.2: Energy dispersive spectroscopy (EDS) of Aluminum 359 alloy

It can be seen from EDS results shown in figure 3.2, the wt % of Al and Si are 86.93 % and 10.22 % respectively. Thereafter the metal *i.e.* Al 359 is used in stir casting furnace for the composite preparation.

3.1.2 Stir casting

The moulds were prepared from green sand for the stir casting process is shown in figure 3.3

Figure 3.3: Preparation of mould for casting

Stir casting process is selected among the different process used for making composite material, because it helps in proper mixing of matrix and reinforcements. In the stir casting process, the

Al-359 alloy was heated in a furnace at about 830°C, which is above the aluminum alloy's melting temperature of 690°C. The calculated quantity of SiC and graphite powder was heated to 300°C, and then fed at a constant rate into the aluminum molten metal. The stir casting machine and process is shown in figures 3.4 and 3.5.

Figure 3.4: Stir casting machine

Figure 3.5: Stir casting process

In order to achieve the optimum mechanical properties, it is essential to achieve the uniform distribution of the SiC reinforcement within the aluminum matrix. From the literature review, it has been decided to stir the molten metal at a speed of 600 rpm for 10 minutes. Also, the depth of immersed impeller is approximately 2/3 of the height of the molten metal from the bottom of crucible. Hence, during the stir casting process, the aluminum molten metal-SiC-graphite slurry was stirred continuously for 10 minutes, by a mechanical stirrer at 600 rpm to disperse the SiC and graphite particles into the melt. A fine vortex was created by the mechanical stirrer. The mechanical stirrer consisted of solid rod and impeller. The material for the rod was stainless steel 304 grade which was purchased from Kalawati Metal House, Patiala and graphite material was chosen for impeller material because of high temperature resistance. It was purchased from Sunrise enterprises, Mumbai. The rod and impeller for stirrer is shown in figure 3.6. During stirring, the molten mixture was poured into the sand moulds. Finally, the molten mixture was allowed to solidify in the moulds to obtain the required plates.

Figure 3.6: Preparation of rod and impeller for stirrer

The steps involved in making of composite using stir casting method are:

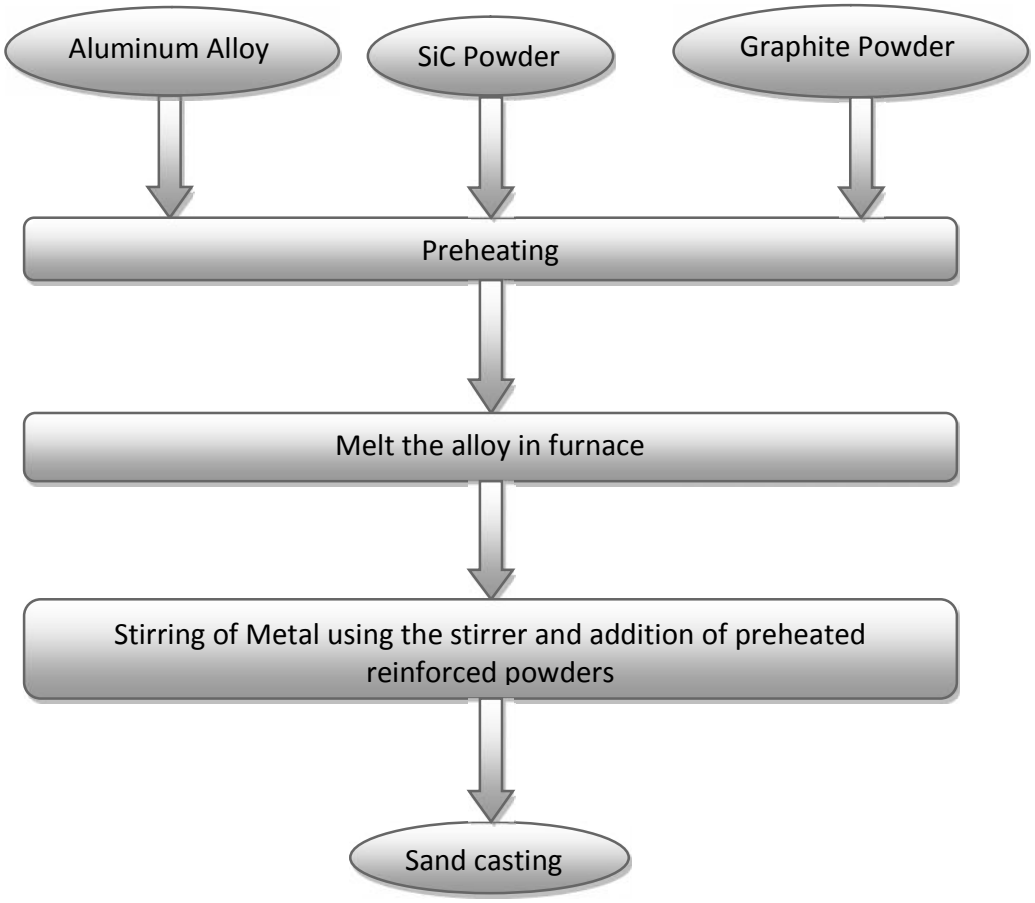

Figure 3.7 Flowchart showing the stir casting process

The ‘as-cast’ condition of the Al 359 alloy, Al 359/SiC and Al 359/SiC/Gr plates are shown in figure 3.8.

Figure 3.8: Al 359 alloy, Al 359/SiC and Al 359/SiC/Gr (7 inch, 14 inch and 21 inch respectively) plates in the ‘as-cast’ condition

3.1.3 Evaluation of Metallurgical properties of prepared composite

- **Evaluation of microstructure**

Metallurgical characterization of prepared MMCs were carried out using a Scanning Electron Microscope (SEM) with Energy Dispersive Spectroscopy (EDS). The specimens prepared from the cast MMCs were polished. The microstructure of specimens were observed and EDS was performed to determine the chemical composition of the matrix and reinforcement formed. The SEM image and EDS of Al with 10 % wt. SiC are shown in figures 3.9 and 3.10.

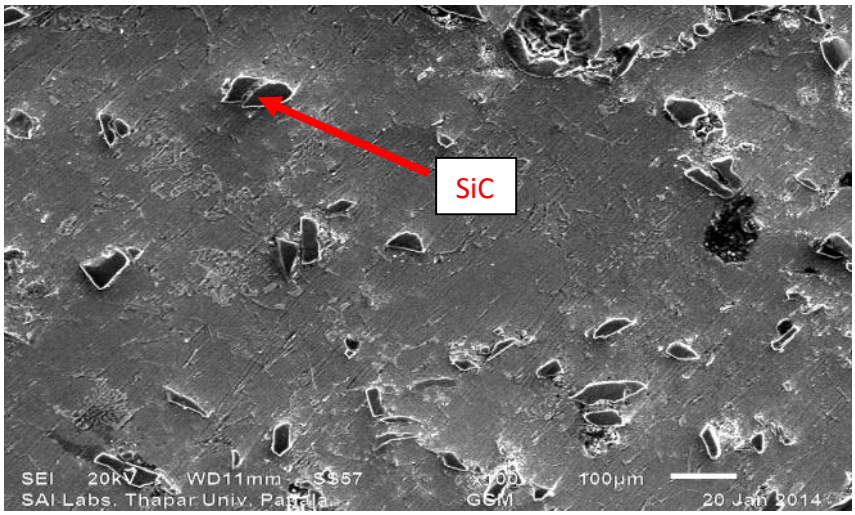

Figure 3.9: SEM image of Al 359 – 10 % wt. SiC MMC

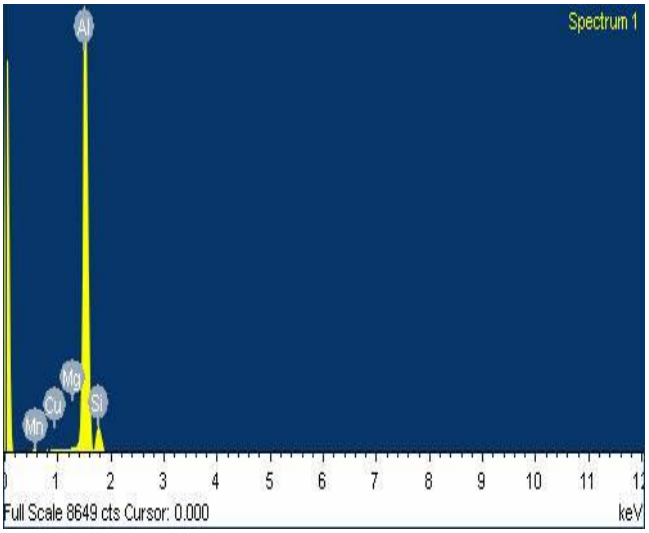

Element	Weight%
Al K	76.40
Si K	11.83
Mn K	0.32
Cu K	0.29
Mg K	0.02
C K	11.14
Totals	100.00

Figure 3.10: EDS of Al 359 - 10% wt. SiC MMC

SEM image shows the uniform dispersion of SiC into Al. The EDS shows the increase in the content of Si and C due to SiC addition.

The SEM image and EDS of Al with 7.5 % wt. SiC and 2.5 % wt. of graphite are shown in figures 3.11 and 3.12.

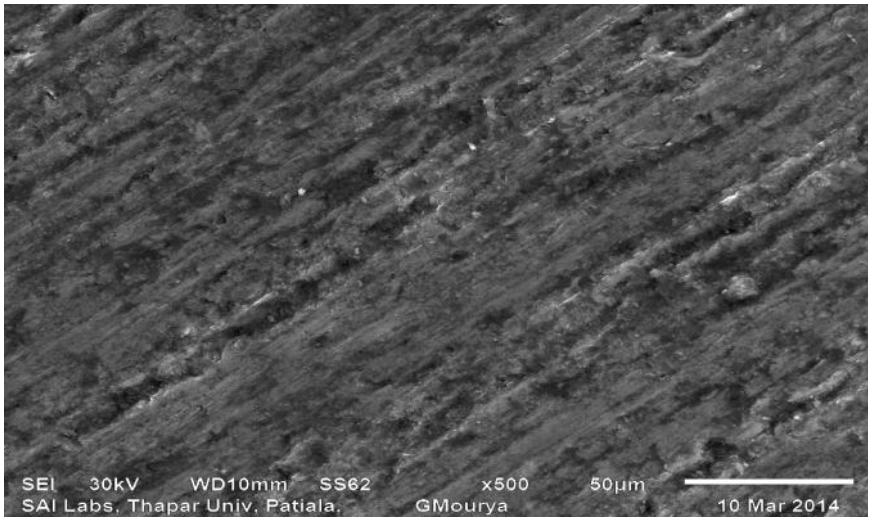

Figure 3.11: SEM image of Al 359 – 7.5% wt. SiC – 2.5% wt. Graphite MMC

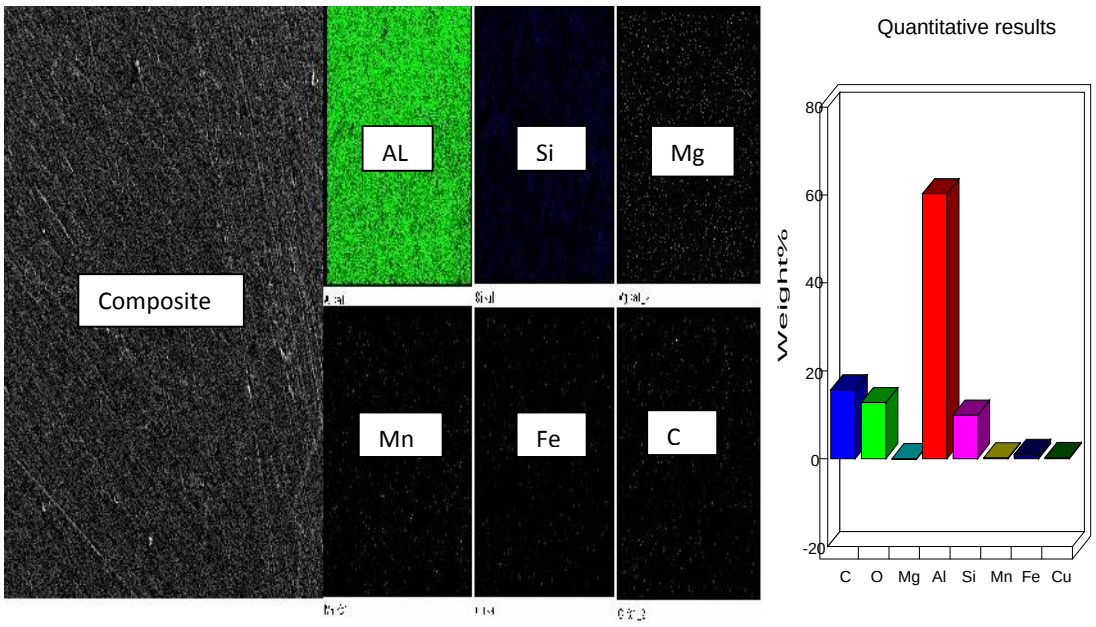

Figure 3.12: EDS of Al 359 – 7.5% wt. SiC – 2.5% wt. Graphite MMC

The figures shows the homogenous dispersion of SiC and graphite reinforcements particles in the aluminum alloy matrix.

3.1.4 Hardness test

To evaluate the hardness of alloy and composites, the Vickers hardness and Rockwell hardness tests were conducted. The macro hardness was measured using Rockwell hardness tester (Avery 6402 Type) shown in figure 3.13 (a) at a load of 100 kgf for a period of 15 seconds. The micro hardness of polished samples were measured at different locations using the Vickers hardness tester (Mitutoyo) at a load of 100 gm. for 10 seconds shown in figure 3.13 (b).

(a) **(b)**

Figure 3.13: (a) Rockwell hardness (b) Vickers hardness tester

The Rockwell hardness test was conducted at Solid Mechanics lab in MED and the Vickers hardness test was conducted at Material Science lab (P.G.) in SPMS, Thapar University, Patiala. The estimated macro and micro hardness of prepared Aluminum alloy and composites are given in Table 3.1.

Table 3.1: Macro and Micro hardness of produced composites

Sr. No.	% of SiC in Al 359 alloy matrix	% of graphite in Al 359 alloy matrix	Macro Hardness (HRB)	Micro Hardness (HV)
1.	0	0	84.67	72.70
2.	10	0	89.00	94.97
3.	7.5	2.5	86.00	85.17

As can be seen from table 3.1 that the macro and micro hardness of 10 % SiC is better than 7.5% SiC/2.5% Gr. The addition of graphite reduces the hardness of composite because it acts as a lubricant.

3.2 Fabrication of FSW joints

The right selection of welding parameters plays an important role in deciding the joint strength of weld which is directly affected by the tool. Hence, the experiments were performed by considering these factors for analyzing the effect of input welding parameters on tool wear.

A vertical milling CNC machine purchased from the Chandra as shown in figure 3.14 is used to fabricate the joint. This is a 3-axis Numerical Controlled machine which is equipped with Automatic Tool Changer. The machine is available in CAM lab of MED, Thapar Univ., Patiala.

Figure 3.14: Full view of CNC vertical milling machine

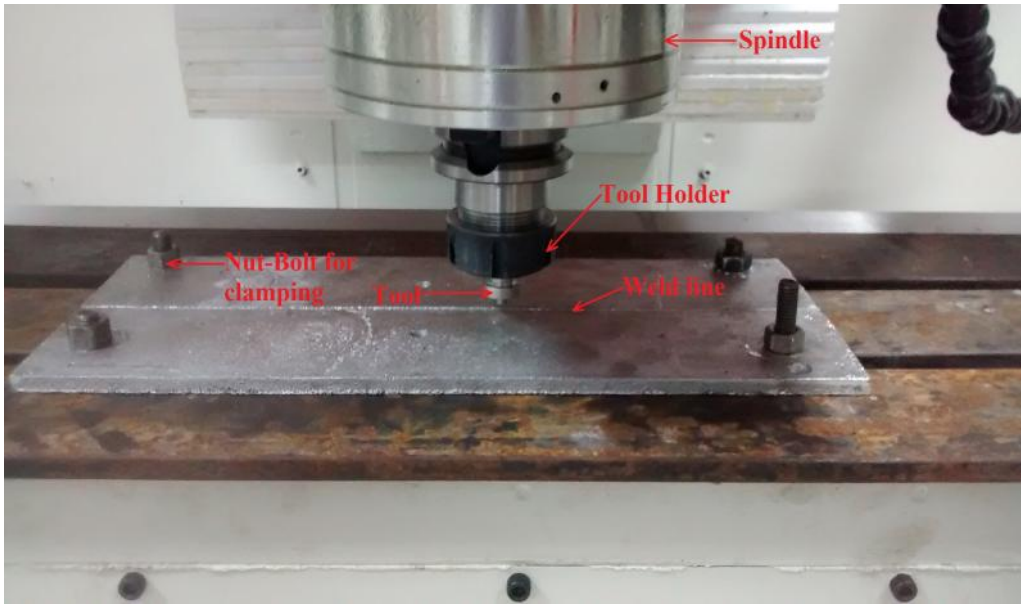

Figure 3.15: Close up view of FSW

The above figure 3.15 shows the set- up of plates and tool on CNC machine for performing the FSW process.

The machine is based on word address format of Manual Part Programming. The program controller of CNC machine with the program is shown in figure 3.16:

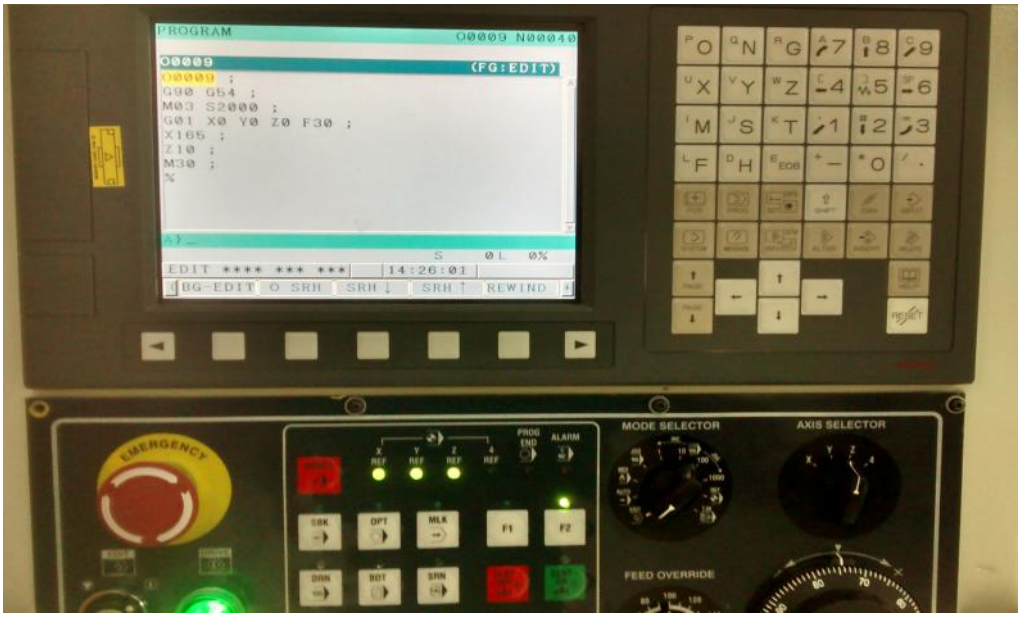

Figure 3.16: Program controller of CNC vertical milling machine

3.2.1 FSW Tool

The tool plays an important role in the FSW process. The tool was used to join the plates. Three tools were prepared for each set of alloys, composites and hybrid composites. The material for the tool is selected to be Stainless Steel 304 grade with composition given in table 3.2. The material is selected due to high temperature strength, corrosion resistance, etc. Shape and size of tool is as following:

- Shoulder and pin diameter to be 18 mm and 6 mm respectively.
- Tool profile to be cylindrical pin with thread pitch of ¼ inch BSW.
- Shoulder and pin length to be 5 mm and 5.5 mm respectively.

The FSW tools are shown in figure 3.17. The form of tool geometry is important factor for producing defect free joints. The tool is fabricated on the center lathe machine and the die is used for creating thread on pin. The macro hardness of the tool is 85 HRC which is measured on the Rockwell hardness machine.

Table 3.2: Composition of Stainless Steel 304 grade (http://www.Stainless Steel - Grade 304 (UNS S30400).htm)

Carbon	0.08 max.
Manganese	2.00 max.
Phosphorus	0.045 max.
Sulfur	0.030 max.
Silicon	0.75 max.
Chromium	18.00-20.00
Nickel	8.00-12.00
Nitrogen	0.10 max.
Iron	Balance

Figure 3.17: FSW tools
(1 for Al 359 alloys, 2 for Al 359 – SiC composites, 3 for Al 359 – SiC – Gr composites)

3.2.2 FSW joints

The plates of 6 mm thickness (Al 359, Al 359 – 10% SiC and Al 359 - 7.5% SiC - 2.5% Gr MMCs) were used into three sizes of alloys, composite and hybrid composite (177 x 70, 355 x 70, 533 x 70 mm) for welding. A butt joint configuration is prepared to fabricate the FSW joints. The joint configuration is obtained by securing the plates in clamping position using nuts and bolts. The direction of welding is normal to the rolling direction. A single pass welding procedure and non-consumable tools made of stainless steel are used to fabricate the joints. The details regarding the welding parameters used to fabricate the joints are presented in Table 3.3.

Table 3.3: Factors and levels for experimental study

Sr. No.	Factors	Units	Level 1	Level 2	Level 3
1.	Rotation Speed	rpm	1000	1500	2000
2.	Traverse Speed	mm/min	20	30	40
3.	Length of weld	inch	7	14	21
4.	Material	-	Al 359 alloy	Al 359 - 10% SiC	Al 359 alloy -7.5 % SiC - 2.5% Gr

After the selection of factors and levels, experimental test are designed. Table 3.4 shows the experimental test matrix design with 3 levels and 4 factors:

Table 3.4: Experimental Test matrix showing parameters variation and no. of experiments

Experiment No.	Factors			
	Rotation Speed (rpm)	**Traverse Speed (mm/min)**	**Length of weld (inch)**	**Material**
1.	1000	20	7	Al 359 alloy
2.	1000	30	14	Al 359 alloy - 10% SiC
3.	1000	40	21	Al 359 alloy- 10% SiC-2.5% Gr
4.	1500	20	14	Al 359 alloy- 10% SiC-2.5% Gr
5.	1500	30	21	Al 359 alloy
6.	1500	40	7	Al 359 alloy - 10% SiC
7.	2000	20	21	Al 359 alloy - 10% SiC
8.	2000	30	7	Al 359 alloy- 10% SiC-2.5% Gr
9.	2000	40	14	Al 359 alloy

After the selection of parameters, experiment is performed on CNC machine. FSW tool is rotated and slowly plunged into the joint line until the shoulder of tool touched the surface of plates to be joined. Sufficient dwell time is allowed to generate frictional heat and the tool is moved along

the weld line. The plasticized material is transferred from leading edge of tool to trailing edge and forged along by the shoulder of tool with applied pressure. Finally, the tool is retracted from the plate. Nine joints are prepared as per the selection of four factors at three levels, to find out the effects of the process parameter on tool wear. One of the fabricated joint is shown in figure 3.18.

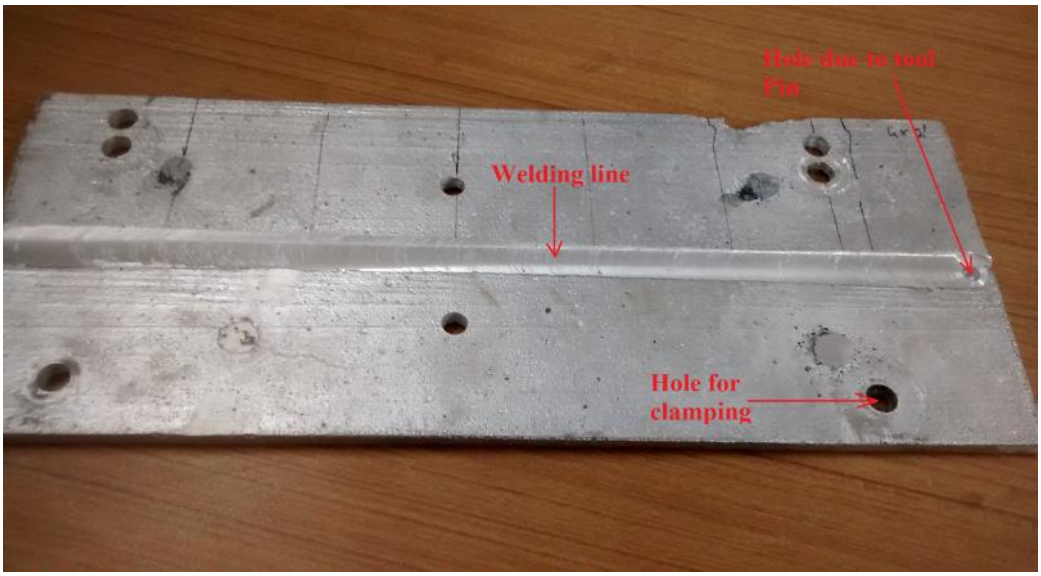

Figure 3.18: Fabricated FSW joints plates

3.2.4 Evaluation of macro hardness of mid-thickness region across the weld

Macro hardness is measured at the mid thickness region across the weld line. The base aluminum alloy has recorded a Rockwell hardness of 84.67 HRB, which is lower than that of the stir zone (SZ). The hardness of the SZ is substantially higher than that of the base aluminum alloy *i.e.* 97.5. Similarly, Al – SiC composite has recorded a Rockwell hardness of 86 HRB which is lower than SZ *i.e.* 103. Al – SiC- Gr hybrid composite has recorded a Rockwell hardness of 89 HRB which is lower than SZ *i.e.* 99. There are two main reasons for the improved hardness of the SZ; (a) the grain size of the SZ is much finer than that of the base metal, grain refinement plays an important role in strengthening of material (b) The small particles of intermetallic compounds also helps good to improve hardness.

CHAPTER 4 Results and Discussions

4.1 Quantifying wear of tool

The tools are used for the nine plate specimens. Each tool corresponds to a particular material *i.e.* alloy, composite and hybrid composite. For the quantification of tool wear, weight loss method is used. Before performing the process, weight of tool is measured using a weighing machine, shown in figure 4.1. During the FSW process, aluminum stuck to the pin of tool. It is necessary to remove the aluminum before measuring the weight. For the removal of aluminum, a solution of 5% NaoH in water is used. Solution is prepared by the dissolving the Sodium Hydroxide Reagent Grade pellets into water. Tool is submerged into solution for 5 hours. Then the weight of tool is measured. The percent of tool wear is calculated using equation (4.1).

$$Percent\ of\ tool\ wear = \frac{Initial\ weight - Final\ weight}{Initial\ weight} \quad (5.1)$$

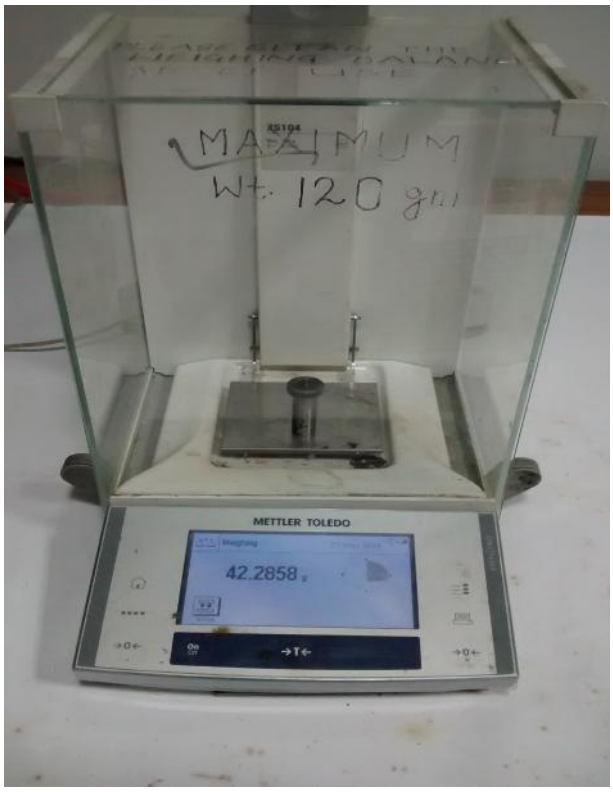

Figure 4.1: Weighing Machine

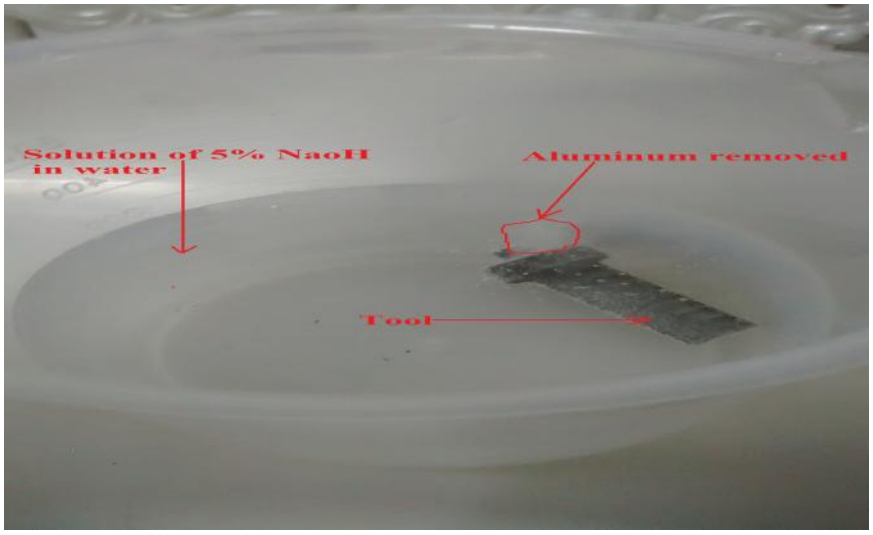

Figure 4.2: Aluminum removal in Solution of 5% NaoH in water

The percent of tool wear calculated for different combination of parameters is given in table 4.1.

Table 4.1: Percentage of tool wear

Experiment No.	Factors				% of Tool Wear
	Rotation Speed (rpm)	Traverse Speed (mm/min)	Length of weld (inch)	Material	
1.	1000	20	7	Al 359 alloy	0.00206
2.	1500	30	21	Al 359 alloy	0.00619
3.	2000	40	14	Al 359 alloy	0.04483
4.	1000	30	14	Al 359 alloy - 10% SiC	0.20022
5.	1500	40	7	Al 359 alloy - 10% SiC	0.06574

6.	2000	20	21	Al 359 alloy - 10% SiC	1.81187
7.	1000	40	21	Al 359 alloy- 10% SiC-2.5% Gr	0.06049
8.	1500	20	14	Al 359 alloy- 10% SiC-2.5% Gr	0.00597
9.	2000	30	7	Al 359 alloy- 10% SiC-2.5% Gr	0.15716

Figure 4.3: Condition of tool (after wear)
(1 for Al 359 alloys, 2 for Al 359 – SiC composites, 3 for Al 359 – SiC – Gr composites)

Figure 4.3 shows the tool condition after wear. It is clear from the figure that maximum wear of tool pin is showing in the tool no. 2. This tool was used for FSW of Al/SiC composite plates. The diameter of pin is drastically reduced in this case. The tool no. 3 showing the maximum wear after the tool no 2. This tool was used for FSW of Al/SiC/Gr composite plates. The tool no. 1 was used for Al alloy which is showing the least wear of tool pin.

Figure 4.4 to 4.6 are the plots of rotational speed, traverse speed and length of weld versus % of tool wear for the Al 359 alloys, Al 359 – SiC composites and Al 359 – SiC – Gr composites respectively.

In the case of rotational speed, maximum tool wear occurs in case of Al 359 – SiC composites at rotational speed of 2000 rpm. But in case of traverse speed, maximum tool wear occurs in case

of Al 359 – SiC composites at minimum rotational speed of 20 mm/min. Finally, in case of length of weld, maximum tool wear occurs in case of Al 359 – SiC composites at maximum length of 21 inch.

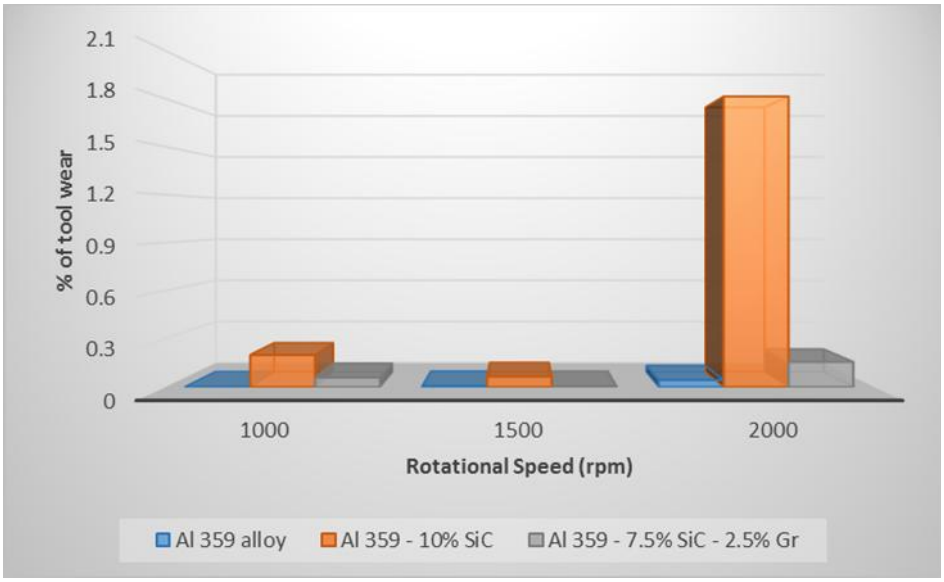

Figure 4.4: Rotational speed vs. % of tool wear

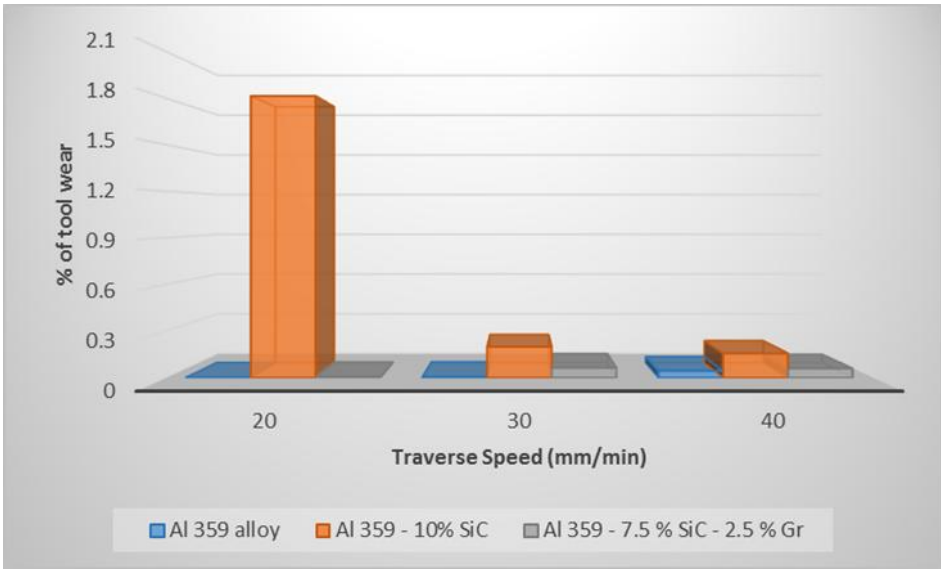

Figure 4.5: Traverse speed vs. % of tool wear

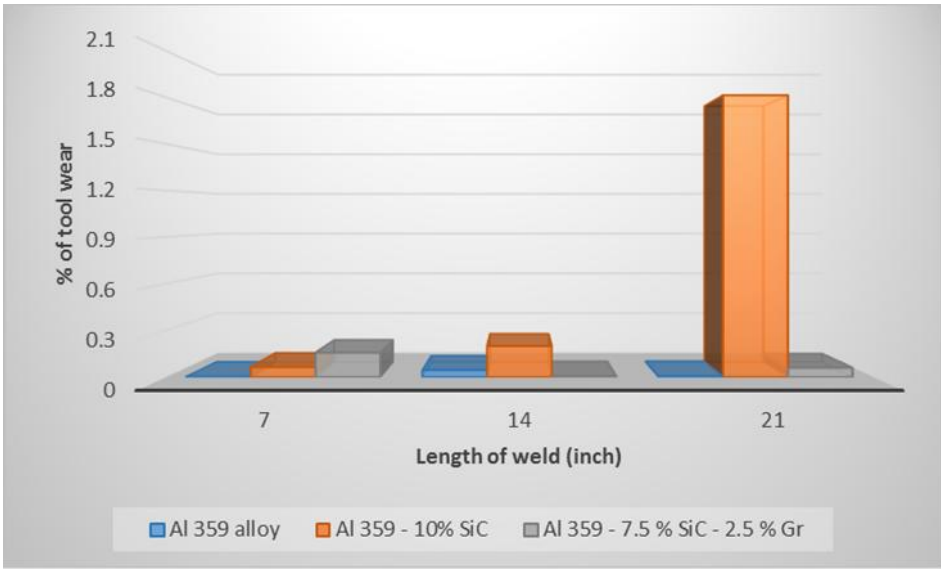

Figure 4.6: Length of weld vs. % of tool wear

4.2 Evaluation of Metallurgical properties of tool

Scanning Electron Microscope (SEM) of tool's pins was done for metallurgical characterization after the FSW was performed on plates. The top and side portion of tool's pin were selected for studying the wear of surface. The following figures 4.7 to 4.9 shows the surface of tool's pin which clearly showing the surface wear of tools.

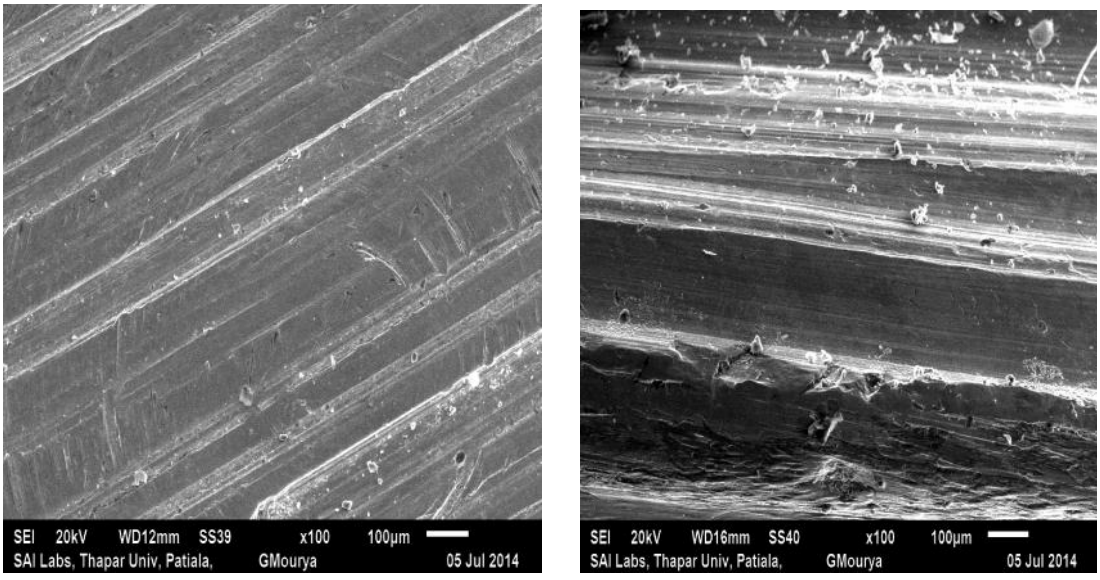

(a) **(b)**

Figure 4.7: SEM image of tool used for FSW of Al alloy plates (a) top portion (b) Side portion

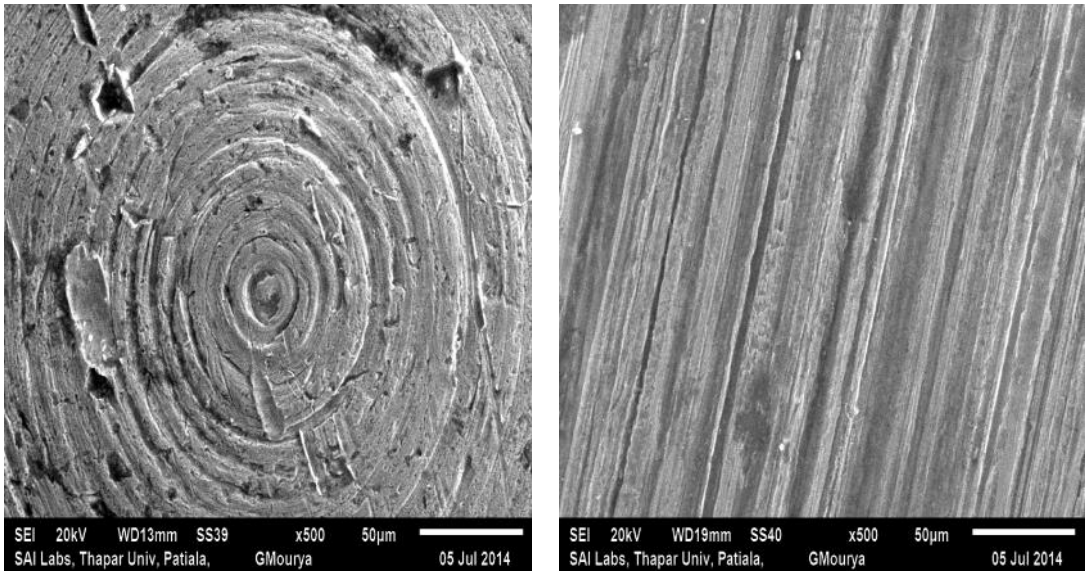

(a) **(b)**

Figure 4.8: SEM image of tool used for FSW of Al-SiC composite plates (a) top portion (b) Side portion

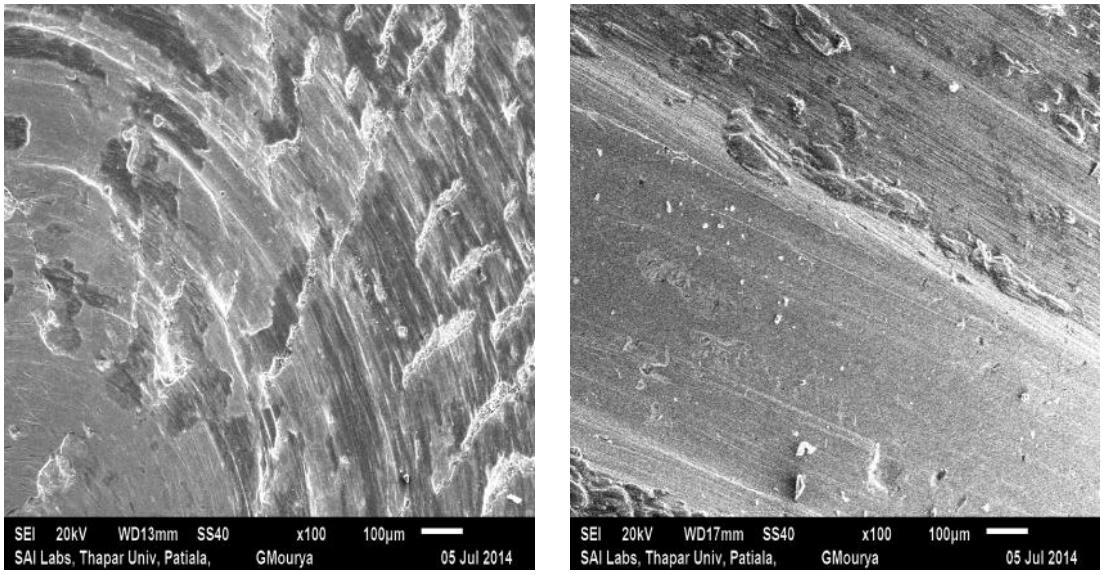

(a) **(b)**

Figure 4.9: SEM image of tool used for FSW of Al-SiC-Gr composite plates (a) top portion (b) Side portion

4.3 Measurement of temperature

During the FSW of the plates, temperature of tool's shoulder was measured with the help of laser thermocouple at particular distance of plates. Laser was focused at a point for measuring of temperature.

Figure 4.10: Measuring of temperature with the help of laser thermocouple

Figure 4.11 to 4.13 shows the plots of temperature of shoulder of tool versus length for the Al 359 alloys, Al 359 – SiC composites and Al 359 – SiC – Gr composites welded.

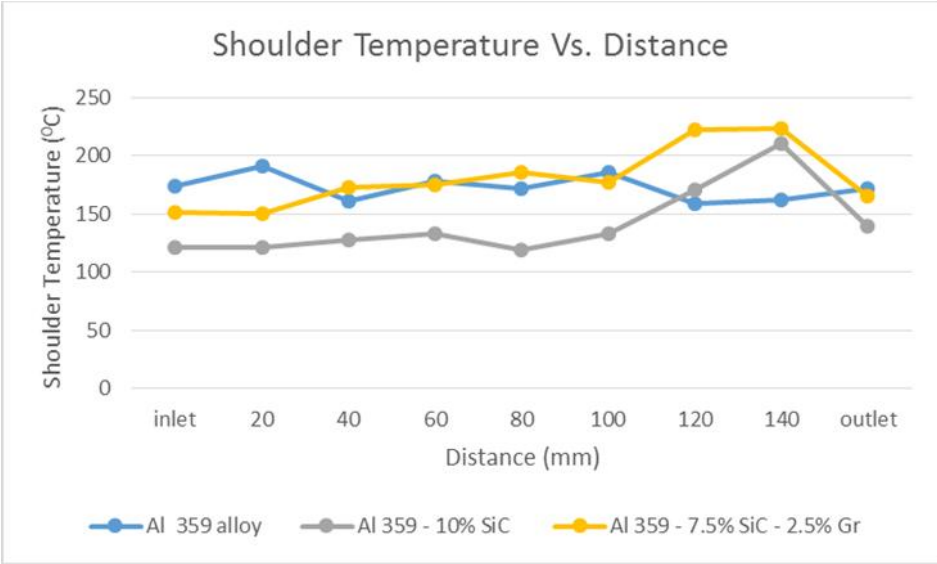

Figure 4.11: Temperature of shoulder versus distance (for 7 inch plate)

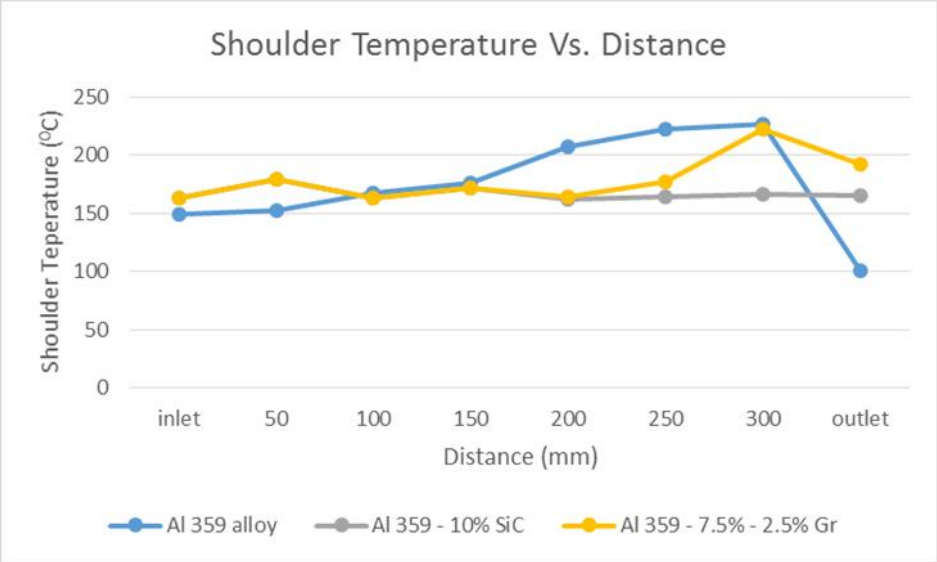

Figure 4.12: Temperature of shoulder versus distance (for 14 inch plate)

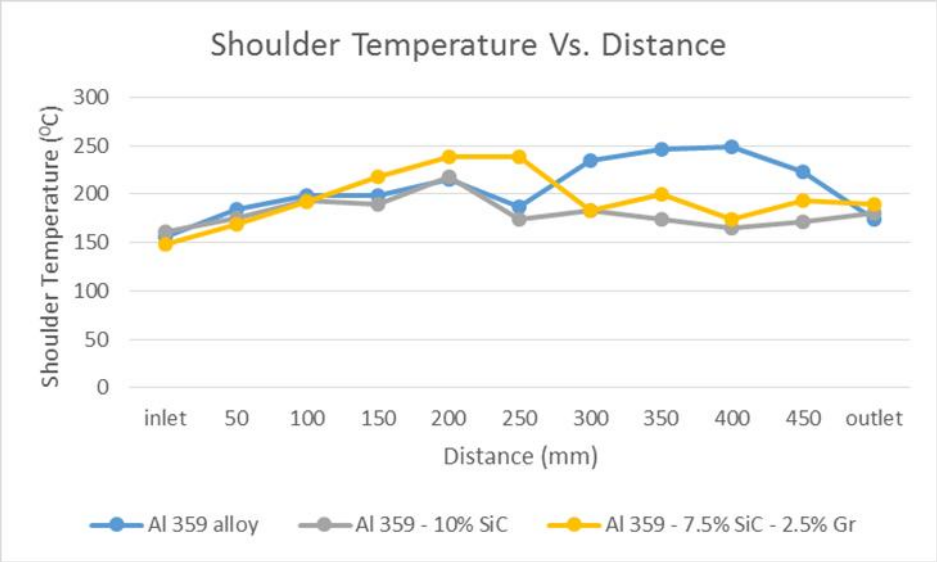

Figure 4.13: Temperature of shoulder versus distance (for 21 inch plate)

Following are the plots of maximum temperatures for the Al 359 alloys, Al 359 – SiC composites and Al 359 – SiC – Gr composites as shown in figure 4.14 to 4.16.

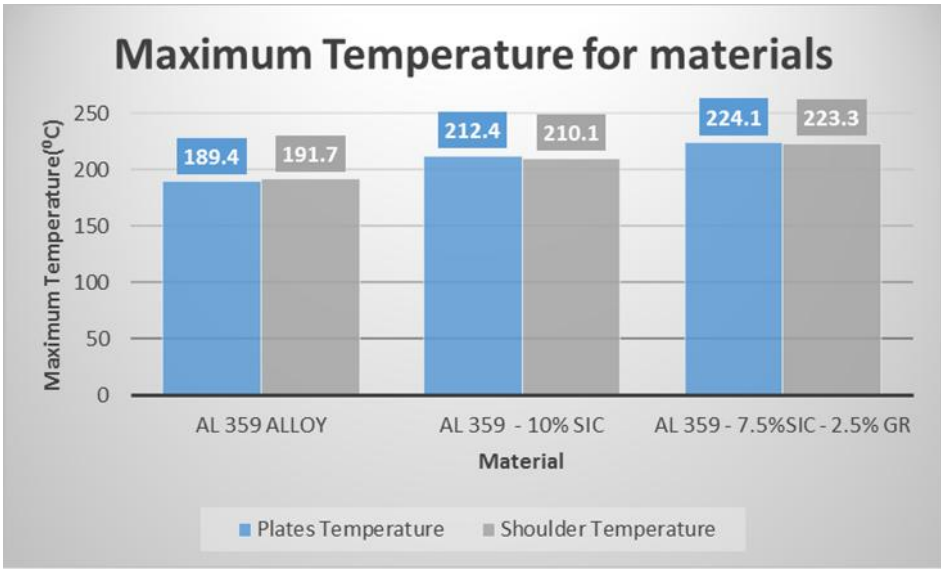

Figure 4.14: Plot for maximum temperature of plates and shoulder for different material (for 7 inch plate)

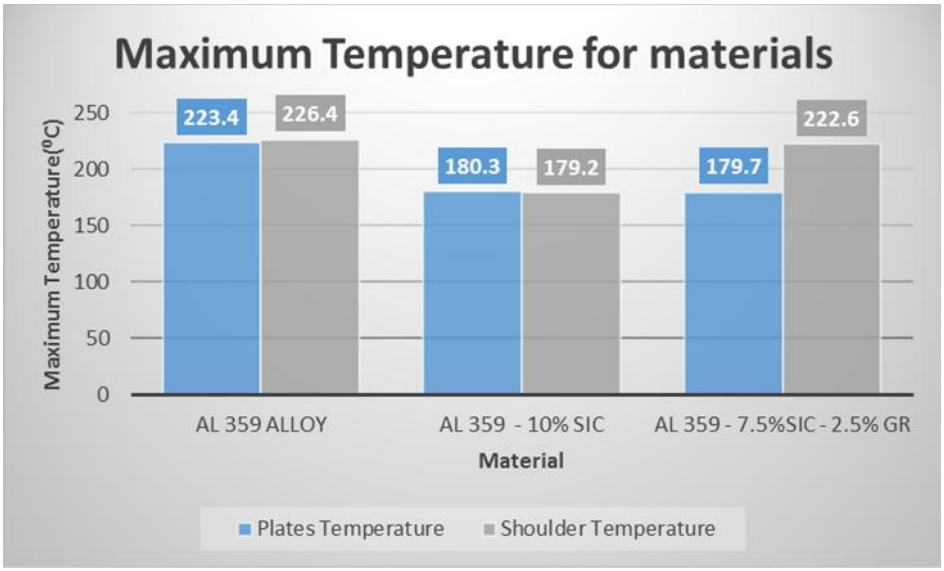

Figure 4.15: Plot for maximum temperature of plates and shoulder for different material (for 14 inch plate)

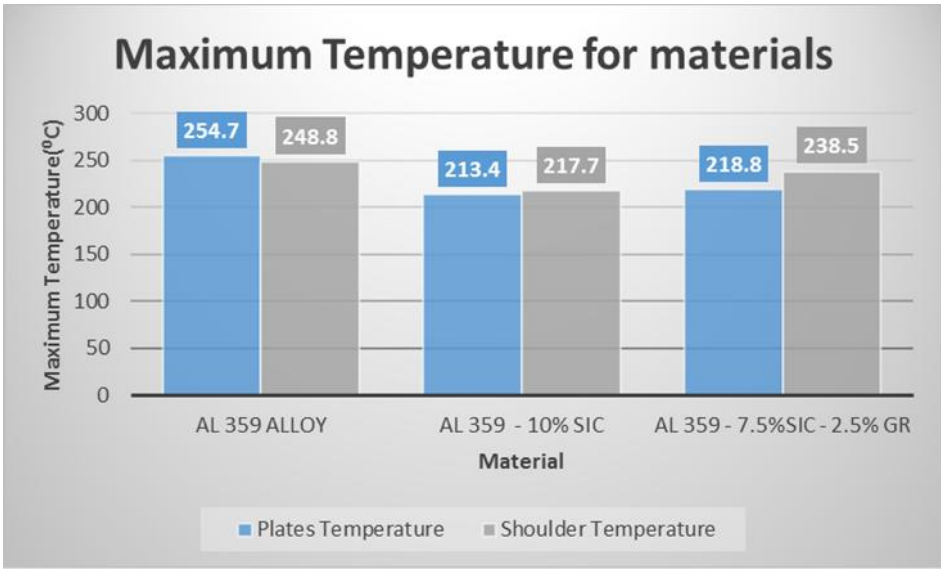

Figure 4.16: Plot for maximum temperature of plates and shoulder for different material (for 21 inch plate)

Peak temperature in the nugget zone directly depends on the weld power, this weld power is directly proportional to temperature at constant traverse speed. Higher weld power is obtained by increasing the rotational speed at constant traverse speed. The highest temperature attained at traverse speed 20, 30 and 40 mm/min and rotational speed of 2000 rpm in three cases of materials were 213.4 ^{0}C, 254.7 ^{0}C and 223.4 ^{0}C respectively.

CHAPTER 5 CONCLUSIONS AND FUTURE SCOPE

5.1 Conclusions

Following conclusions are drawn after studying the results obtained Al 359 alloy, Al 359 – 10% SiC and Al 359 – 7.5% SiC – 2.5% Gr:

- Stirring time and speed plays an important role in the uniform distribution of reinforced particles in the matrix.
- By comparing the amount of tool wear, maximum tool wear occurred in welding of Al 359 – 10% SiC composite, due to presence of SiC reinforcement particles.
- Tool wear occurred in case of Al 359 – 7.5% SiC – 2.5% Gr is less than Al 359 – 10% SiC composite due to addition of graphite reinforced particles which acts as a lubricant in composite and makes the composite softer.
- High surface finish can be obtained at low traverse speed and high rotational speed.
- Rigid clamping of the plates is necessary for the good quality of weld because higher vibration are produced during FSW.
- Dry run for the alignment of tool with welding line of plates is necessary to obtain a sound weld with excellent mechanical properties.

5.2 Scope for future work

Following studies can be considered for the future work:

- õ Reinforced particles with different particle sizes can be used to study the effect of size of particles on the properties of composites.
- õ Dissimilar materials can be used for performing the FSW process using the different parameters.
- õ To study the tool wear, different tool profiles can be tried.
- õ Different tool materials can be used for study.
- õ The finite element method can be used to study the effect of temperature on different zones of weld.

REFERENCES

[1] Iseki T., Kameda, T., Maruyama T., "Interfacial reactions between SiC and aluminium during joining", *Journal of Materials Science*, 19 (5), 1692-1698, 1984.

[2] Thomas W. M., Nicholas E. D., Needham J. C., Murch M. G., Templesmith P., Dawes C. J., "Friction stir butt welding", G. B. Patent Application No 9125978.8, 1991.

[3] Dahotre N. B., McCay M. H., McCay T. D., Gopinathan S., Allard L. F., "Pulse Laser Processing of a SiC/Al-Alloy Metal Matrix Composite", *Journal Of Material Research*, 6 (3), 514-29, March 1991.

[4] Ellis, M.B.D., Gittos M. F., Threadgill, P.L., "Joining Aluminum based metal matrix composites", *Materials World*, 8, 415–417, 1994.

[5] Hashim J., Looney L., Hashmi M. S. J., "Metal matrix composites: production by the stir casting method", *Journal of Materials Processing Technology*, 92/93, 1-7, 1999.

[6] Mendez F. Patricio, Eagar, Thomas W., "New Trends in Welding in the Aeronautic Industry", *New Trends for the Manufacturing in the Aeronautic Industry*, 2000.

[7] NASA, *Friction Stir Welding, Space Shuttle Technology Summary*, http://www.nasa.gov/centers/marshall/pdf/104835main friction.pdf, 2001.

[8] Prado R. A., Murr L. E., Shindo D. J.; Soto K. F., "Tool wear in the friction-stir welding of aluminum alloy 6061 + Al2O3: a preliminary study", *Scripta Materialia*, 45(1), 75– 80, 2001.

[9] Sharma Pardeep, Chauhan Gulshan, Sharma Neeraj, "Production of AMC by stir casting – An overview", *International Journal of Contemporary Practices*, 2 (1), 23-46, 2001.

[10] Kunze J. M., Bamptom C. Clifford, "Challenges to developing and producing MMCs for space applications", *Journal of the Minerals, Metals and Material Society*, 53(4), 22-25, 2001.

[11] Shindo D. J., Rivera A. R., Murr L. E., "Shape optimization for tool wear in the friction stir welding of cast Al 359-20% SiC reinforcement", *Journal of Materials Science*, 37(23), 4999–5005, 2002.

[12] Prado R. A., Murr L. E., Soto K. F. and McClure J. C., "Self-optimization in Tool wear for friction-stir welding of Al 6061+20%Al2O3", *Materials Science and Engineering*, 349 (1), 156-165, May, 2003.

[13] Fernandez G. J., Murr L. E., "Characterization of tool wear and weld optimization in the friction-stir welding of cast aluminum 359+20% SiC metal matrix composite", *Materials Characterization*, 52 (1), 65-75, March 2004.

[14] Storjohann D., Barabash O. M., David S.A., Sklad P.S., Bloom E. E., Babu S.S., "Fusion and Friction Stir Welding of Aluminum Metal Matrix Composites", *Metallurgical and Materials Transactions A*, 36(11), 3237–3247, 2005.

[15] Liu F. J., Feng J. C., Fujii H., Nogi K., "Wear characteristics of a WC-Co tool in friction stir welding of AC4A+30% vol. SiCp composite", *International Journal of Machine Tools and Manufacture*, 45 (14), 1635-1639, 2005.

[16] Rowe C.E.D., Wayne Thomas, "Advances In Tooling Materials for Friction stir Welding", *Cedar Metals Ltd, TWI Cambridge*, 1-11, 2005.

[17] Mishra S. Rajiv, Ma ZY, "Friction stir welding and processing", *Materials Science and Engineering: R: Reports*, 50(1), 1-78, 2005.

[18] Gharacheh Abbasi M., Kokabi H.A., Daneshi H.G., Shalchi B., Sarrafi R., "The influence of the ratio of ''rotational speed/traverse speed'' (ω/v) on mechanical properties of AZ31 friction stir welds", *International Journal of Machine Tools & Manufacture*, 46(15), 1983–1987, 2006.

[19] Prabu S. Balasivanandha, Karunamoorthy L., Kathiresan S., Mohan B., "Influence of stirring speed and stirring time on distribution of particles in cast metal matrix composite", *Journal of Materials Processing Technology*, 171, 268-273, 2006.

[20] Shercliff H. R., Colegrove P. A., "Development of Trivex friction stir welding tool part 2: three-dimensional flow modeling", *Science and Technology of Welding and Joining*, 9 (4), 352-361, 2006.

[21] Threadgill P.L., "Terminology in friction stir welding", *Science and Technology of Welding and Joining*", 12(4), 357-360, 2007.

[22] Prater T., Cook G.E., Strauss A.M., Davidson J., Howell M., "Parameterization of Friction Stir Welding of Al 6061/SiC/17.5p for Various Tool Materials", *8th International Conference on Trends in Welding Research, Pine Mountain, GA*, 2008.

[23] Singla Manoj, Dwivedi D. Deepak, Singh Lakhvir, Chawla Vikas, " Development of aluminum based silicon carbide particulate metal matrix composite", *Journal of Minerals Characterization & Engineering*, 8 (6), 455-467, 2009.

[24] Jayaraman M., Sivasubramanian R., Balasubramanian V., Lakshminarayanan A. K., "Optimization of process parameters for friction stir welding of cast aluminum alloy A319 by Taguchi method", *Journal of Scientific & Industrial Research*, 68, 36-43, January 2009.

[25] Biswas P., Mandal R. N., "Experimental study on friction stir welding of marine grade aluminum alloy", *Journal of Ship Production*, 25, 1-6, 2009.

[26] Zhang Z., Liu Y. L., Chen J. T., "Effect of shoulder size on the temperature rise and the material deformation in friction stir welding", *International journal of Advanced Manufacturing Technology*, 45, 889-895, 2009.

[27] Prater T.J., Strauss A.M., Cook G.E., Machemehl C., Sutton P., Cox C.D., "Statistical Modeling and Prediction of Wear in Friction Stir Welding of a Metal Matrix Composite (Al 350/SiC/20p)", *Journal of Manufacturing Technology Research*, 2(1/2), 1–13, 2010.

[28] Sinclair C.Paul, Longhurst R.William, Chase D.Cox, David H. Lammlein, Alvin M. Strauss, George E. Cook, "Heated Friction Stir Welding: An Experimental and Theoretical Investigation into how Preheating Influences on Process Forces", *Materials and Manufacturing Processes*, 25(11), 1283-1291, 2010.

[29] Balasubramanian V., "Friction stir welding: an environmentally cleaner welding process",http://www.iiwindia.com/pdf/Placid%20Rodriguez%20Memoial%20Lecture-2010-%20Dr%20V%20Balasubramanian-%2028-12-2010.pdf, 2010.

[30] Prater Tracie, "Solid-State Joining of Metal Matrix Composites: A Survey of challenges and Potential Solutions, *Materials and Manufacturing Processes*, 26(4), 636–648, 2011.

[31] T. Prater, C. Cox, B. Gibson, A. Strauss, G. Cook, Dimensional Analysis and a Potential Classification Algorithm for Tool Wear in Friction Stir Welding of Metal Matrix Composites, *Proceedings of the Institution of Mechanical Engineers, Part C: Journal of Mechanical Engineering Science*, 226(11), 2759–2769, 2012.

[32] Sidhu Singh Mandeep, Chatha Singh Sukhpal, “Friction stir welding – Process and its variables: Review”, *International Journal of Emerging Technology and Advanced Engineering*, 2(12), December, 2012.

[33] Palanivel R., Mathews Koshy P., Murugan N., Dinaharan I., “Prediction and optimization of wear resistance of friction stir welded dissimilar aluminum alloy”, *Procedia Engineering*, 38, 578-584, 2012.

[34] Hassan Mahmood Adel, Almomani Mohammed, Qasim Tarek, and Ghaithan Ahmed, “Effect of Processing Parameters on Friction Stir Welded Aluminum Matrix Composites Wear Behavior”, *Materials and Manufacturing Processes*, 27(12), 1419–1423, 2012.

[35] Prater Tracie J., Strauss Alvin M., Cook George E., Gibson Brian T., Cox Chase D., “A phenomenological model for tool wear in friction stir welding of metal matrix composites”, *Journal of Metallurgical and Materials Transactions A,* April, 2013.